JOURNAL
of the
OPTICAL SOCIETY
OF AMERICA

VOLUME 22
No. 10

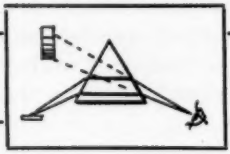

OCTOBER
1932

THE ULTRAVIOLET TRANSMISSION COEFFICIENT OF THE EARTH'S ATMOSPHERE

By R. S. Rockwood and R. A. Sawyer
[University of New Mexico and University of Michigan.
Received July 16, 1932]

ABSTRACT

Thermocouple measurements have been made at four different altitudes in the neighborhood of Albuquerque, New Mexico, of the intensity of solar radiation transmitted by a silver filter. These have been used to determine values of the transmission coefficient defined by $I = Ia^m$ where I and I_0 are respectively the observed and incident energies, a the transmission coefficient and m the air mass traversed in units of the vertical air path directly overhead at sea level and normal pressure. The results, corrected by the use of Hann's empirical equation for the effect of water in the path, gave for a at 3140 m, 0.47; at 2059 m, 0.47; at 1769 m, 0.46; and at 1556 m, 0.43. The last result, from observations on the New Mexico campus is low probably because of dust scattering; the others are in agreement within the errors. The theoretical value calculated from Rayleigh's law of molecular scattering, and using a new value (λ3240) for the wave length of maximum solar energy transmitted by a silver film, is 0.479. The conclusion is, that at least above 1700 m altitude, and for clean dry air, the Rayleigh law for pure molecular scattering is adequate to account for the atmospheric depletion of solar radiation in the silver transmission band. The somewhat discordant results of earlier investigators are discussed.

I. Introduction

The solar radiation which reaches the surface of the earth is weakened in intensity by its passage through the atmosphere. A study of the nature of the various causes of depletion and of their relative significance

has commanded much interest and a large amount of data has been obtained by various workers. For the visible part of the solar spectrum the previous data seem satisfactory; in the ultraviolet, however, the various observations are highly discordant. The aim of the present work has been to obtain additional data in the ultraviolet with the object of throwing further light upon the variations in the existing measurements.

The chief causes of depletion of solar radiation in the atmosphere are: (1) absorption by water vapor; (2) absorption by gases of the atmosphere; (3) scattering by dust and haze; (4) scattering by water vapor; (5) scattering by air molecules.

The absorption by water vapor and by gases is of interest chiefly in the ultraviolet, where ozone and oxygen cause absorption and in the red where the great water vapor bands set in. In the region from λ3000 to λ5000 absorption is a negligible factor in the weakening of the sun's radiation.

The scattering by water vapor and dust is nearly independent of wave length as may be seen from the white color of clouds and haze. The amount of water vapor in the air may be measured and its influence corrected for. The effect of haze is a residual factor after others have been removed. In the present work where interest was centered largely on the molecular scattering, haze scattering was avoided by observing only on the clearest days.

The law of molecular scattering was given by Lord Rayleigh[1] from consideration of an elastic solid theory, and later on the basis of the electromagnetic theory of light. According to this scattering formula the intensity of light after passage through a gas is given by

$$I = I_0 e^{-kx} \tag{1}$$

where I is observed intensity of light of wave length λ; I_0, intensity incident on the medium; X, thickness of the medium; $k = 32\pi^3(\mu-1)^2/3N\lambda^4$; μ, index of refraction of the gas; N, number of gas molecules per unit volume, λ, wave length of incident light.

Many tests have shown that this formula satisfactorily explains the scattering of light by gases in general and by the atmosphere for visible light. Fowle[2] at the Mt. Wilson Observatory, has made extensive observations on the intensity of the solar radiation at all wave lengths from λ3700 to λ17,000. The amount of water vapor was carefully measured and its effect eliminated. The results showed conclusively that in

[1] Rayleigh, Phil. Mag., *47*, 375; 1899.
[2] Fowle, Astrophys. J., *38*, 392; 1913.

the region from λ3700 to λ5000, where there were no absorption effects, that the Rayleigh scattering formula was adequate to account completely for the depletion of the solar radiation by clean dry air. In the region of shorter wave lengths, however, the experimental data are not in entire agreement. The classical investigations of Fabry and Buisson[3] have shown that a strong absorption, which sets in about λ3100, increases rapidly with decreasing wave length and limits the sun's spectrum at about λ2900, may be explained as due to a layer of about 3 mm of ozone in the earth's atmosphere—probably at high altitudes since very little ozone is observed near the earth's surface.[4] Between λ3100 and λ3700 the question as to whether or not Rayleigh scattering is adequate to account for the depletion of solar radiation by pure dry air has received varying and quite discordant answers. Dawson, Granath, and Hulbert[5] by a photographic method measured the absorption of the atmosphere for a 400 m path near the ground and found the Rayleigh formula sufficient to account for all weakening of intensity for wave lengths longer than λ2900. On the other hand Schaeffer[6] who also measured the atmospheric absorption by a photographic method for horizontal air paths near the earth, ranging in length up to 8000 m, found that for wave lengths shorter than λ3400 the Rayleigh scattering alone called for a greater transmission than observed. The chief study of the depletion of solar radiation in this region is that of Pettit[7] who on the basis partly of his own observation and partly on the analysis of those of others concluded that for the light near λ3200, transmitted by a silver filter, the Rayleigh scattering calls for less transmission than actually observed at altitudes above 1800 m, and for greater at lower altitudes. None of these ultraviolet researches took account of the effects of water vapor or dust in the atmosphere which would decrease the expected transmission and thus might account for results in which the observed transmission was less than calculated.

To attempt a further study of the role of Rayleigh scattering in atmospheric transmission the present study was undertaken in the neighborhood of the University of New Mexico at Albuquerque. Using a method similar to Pettit's but correcting for water vapor scattering the coefficient of transmission of the atmosphere for that part of the

[3] Fabry and Buisson, Astrophys. J., *54*, 297; 1921.
[4] Götz and Ladenburg, Naturwiss. *18*, 373; 1931.
[5] Dawson, Granath and Hulbert, Phys. Rev. *34*, 136; 1929.
[6] Schaeffer, Proc. Amer. Acad. of Arts and Sci. *57*, 385; 1921.
[7] Pettit, Nat. Research Council Bull., No. *61*, 101; 1927.

solar spectrum transmitted by a silver film has been determined from measurements made at altitudes of 1556 m, 1769 m, 2059 m, and 3140 m.

Climatic conditions in the southwestern United States are unusually favorable for such a study. High altitude, low humidity, cloudless skies and freedom from the dust of large cities make the atmosphere remarkably clear. In the fall and winter months there are few high winds which might raise dust in the air and so cause loss of radiation by dust scattering. At Albuquerque, New Mexico and in the nearby mountains are found altitudes accessible in an automobile that range from 1556 m (5100 feet) on the campus of the University of New Mexico to 3140 m (10,300 feet).

Albuquerque is situated on the east bank of the Rio Grande at an altitude of about 5000 feet. From the University campus east of the city the mesa slopes gradually and uniformly eastward for a distance of about 8 miles to the base of the Sandia Mountains where the altitude is 6000 feet. The west side of the mountains or the side facing Albuquerque is precipitous, the altitude changing in a horizontal distance of 2 miles to 10,300 feet. The eastern slope is not so steep and here a forest service road leads to the crest of the range. The stations at which observations were made are located *A* at the crest of the range, altitude 10,300 feet; *B* on the west side of the mountain, altitude 6750 feet; *C* on the open mesa, altitude 5800 feet; and *D* on the campus of the University of New Mexico, altitude 5100 feet. Between these stations there is little difference in the character of the country which is semi-arid to arid. The rainfall in Albuquerque varies from 4 to 10 inches per year, a large part of which falls in the months of July and August. In the mountains there is a slightly larger amount of precipitation but in the fall almost no rain falls and the prevailing winds which blow from the desert keep the humidity low.

II. EXPERIMENTAL DETAILS

A diagram of the equipment is shown in Fig. 1. It consisted of a thermopile, *D* located at one end of a brass cylinder of such length that a quartz lens, *B*, at the other end would focus incident radiation on one junction. In the path of the ray between the lens and thermopile was placed a quartz disk, *C*, on one side of which a thin silver film had been deposited by sputtering. The brass cylinder carrying the lens and thermopile was placed inside a Dewar flask, *E*, to reduce errors arising from changes in temperature of the air. This element was inclosed in a

hard rubber cylinder, *F*, as a protection against breakage. Over a window in one end of the protective casing was placed a "Corex A" glass filter, *A*, which also had a thin silver film on its inner side, to insure against unfiltered radiation through possible pin holes in either silver film. The "Corex A" filter was used as an additional filter to keep all longer wave-length radiation out of the equipment. The casing was provided with a finder to insure the proper focusing of the radiation on the junction of the thermopile and the whole unit was given a polar mounting on the base of a heliostat. A Leeds and Northrup high sensitivity galvanometer measured the thermoelectric currents.

To avoid any depletion due to haze, observations were taken only on days when the sky was free from clouds and when the mountains to the north, west, and south, whose distances were from 65 to 100 miles,

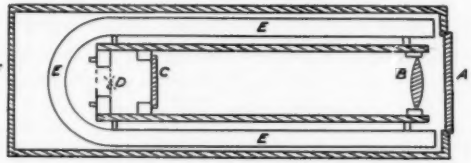

FIG. 1. *Cross section of receiver: A, silvered Corex filter; B, quartz lens; C, silvered quartz plate; D, thermocouple; E, Dewar flask; F, hard rubber case.*

gave a sharp outline against the sky. Observations were begun by 10:00 A.M. if possible and were continued at half hour intervals until 3:30 P.M. For each observation from three to six readings were made, the number of readings taken depending on the agreement of the results. Focusing of the sun's image on the thermopile was accomplished by slowly shifting the receiving set so that the image of the sun moved across the junction of the thermopile. The maximum deflection of the galvanometer was taken as the reading. The zero reading of the galvanometer was observed before and after each exposure and the mean taken for the zero of the reading. Since small changes in the leveling would result in a serious difference of deflection the galvanometer was leveled with a small spirit level and the leveling checked several times each day. Difference in temperature in the galvanometer parts were guarded against by a covering of corrugated card board which completely covered the galvanometer except for a small window left to enable deflections to be observed. At intervals of about one hour readings were taken of the temperatures on the wet and dry bulb thermometers.

A total of 119 observations on 19 days were made at the station on the

campus of the University of New Mexico, elevation 1556 m; 15 on two days at Sunset View Gas Station, elevation 1769 m; 81 on 12 days at Carlito Springs, elevation 2059 m; 54 on 5 days at Kiwanis Cabin, elevation 3140 m.

Table 1 is a typical set of observations and computed results that was made at elevation 1556 m, October 17, 1931.

TABLE 1. *Observations and reduced data for October 17, 1931. Elevation 1556 m, University of New Mexico Campus.*

Hour	Zenith distance ϕ	Air mass $(B/B_0)\sec\phi$	Galvanometer deflection d	Relative intensity $I=dc$	Log I
10:30	47.85°	1.25	6.78	140.3	2.1483
11:00	45.5°	1.19	6.80	140.7	2.1483
11:30	44.2°	1.17	6.98	144.8	2.1608
12:00	43.85°	1.17	6.26	130.0	2.1139
1:30	49.5°	1.29	5.00	103.0	2.0128
2:00	53.35°	1.40	4.66	96.0	1.9823
2:30	57.6°	1.56	4.09	83.5	1.9217
3:00	62.4°	1.81	3.08	63.0	1.7993

Barometer reading, 63.6 cm. Vapor pressure, $e=0.557$ cm. c, a constant.

ANALYSIS OF DATA

For comparison with the results of others it is somewhat more convenient to calculate from the data not the absorption coefficient, k, of Eq. (1) but the transmission coefficient of the atmosphere defined by

$$I = I_0 a^m \tag{2}$$

where "a" is the transmission coefficient and m is the air mass traversed by the light in terms of unit air mass. The unit air mass is the thickness of the atmosphere directly overhead at sea level and at normal atmospheric pressure. This definition differs from one often used in which a unit air mass is defined for each altitude as the air thickness directly overhead at normal pressure. According to our use of the term, for elevations above sea level, the fractional part of the unit mass directly overhead would be given by the ratio B/B_0, of the observed barometric pressure to standard sea-level pressure. Since outside the tropics observations on the sun directly overhead can never be made, the mass of the air traversed by the transmitted radiation is greater than the mass directly overhead by an amount which can be found by multiplying the overhead mass by the secant of the sun's zenith distance, ϕ.

This calculation rests on the assumptions that the portion of the earth's surface is flat and that the layers of air are horizontal, which for a body the size of the earth leads to no large errors for angles up to 75°. The air mass for any barometric pressure and zenith distance is thus

$$m = (B/B_0) \sec \phi. \tag{3}$$

For the calculation of the air mass both the barometric pressure and the sun's zenith distance are required. A small aneroid barometer whose readings were checked with a weather bureau standard mercurial barometer was used to get the barometric pressure. Use of the following equation was made to determine the zenith distance of the sun.

$$\sin h = \sin B \sin \theta + \cos B \cos \theta \cos \alpha$$

h, altitude of the sun; B, latitude of the station; θ, declination of the sun; α, hour angle of the sun. The zenith distance, ϕ, is equal to $90° - h$.

In this formula only B, the latitude of the station, is known directly but both θ and α are obtainable with the help of a nautical almanac.

Eq. (2) may be written in logarithmic form

$$\log I = \log I_0 + m \log a. \tag{4}$$

If $\log I$ be plotted against m the points should fall on a straight line of slope $\log a$ which extrapolated to zero air mass would give the value of I_0, the incident energy. "a" is not quite a constant but for clean air is really the product of two coefficients,

$$a = a_a \cdot a_w^q. \tag{5}$$

Where a_a is the transmission coefficient for dry air and a_w is that for water vapour with exponent q—the thickness in centimeters of the layer of water which would be formed by the precipitation of the water vapor in unit air path.

a_w is for our observations small and study of the data has shown that for purposes of determining I_0 it is sufficiently accurate to regard a as constant. The straight lines so determined by plots of Eq. (4) all lead to the same values of I_0 within the errors of observation. Fig. 2 shows these lines for observations at altitudes 1556 m and 2059 m. The value of I_0 so fixed is of course in arbitrary units of the galvanometer deflections, that is, it is the galvanometer deflection which would be obtained with our apparatus if it could be placed outside the atmosphere.

Using this value of I_0 a value may be calculated for "a" for each observation. To obtain a_a (Eq. (5)) it is necessary to correct for the scat-

tering by water vapor and hence to know the amount of water in the air path. To determine the amount of water present, we have used the empirical equation devised by Hann[8] to fit observations made, at many localities and elevations, of the rate of decrease of vapor pressure with altitude. Naturally it holds only for average conditions. We believe, however, that the steady atmospheric conditions at Albuquerque in the fall with prevailing winds from the desert justify the application of the formula. The vapor pressures, however, were at all times so low

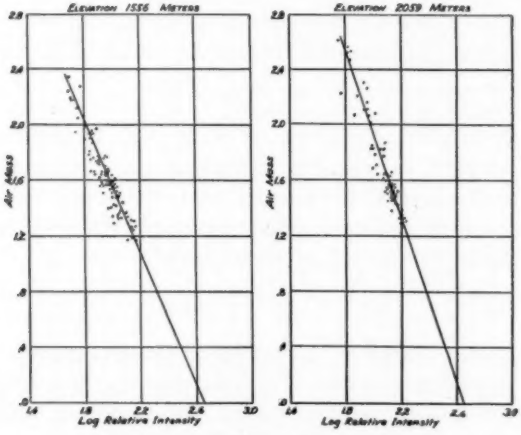

FIG. 2. *Intensity-air mass curves.*

that the correction for water is small and a large uncertainty here would affect the final result only slightly.

Hann's equation is

$$Q_1 = 2.3e_0(1 - 10^{-h/5000}) \tag{6}$$

where d_1 is the quantity of water expressed in cm of precipitable water between sea level and altitude h given in meters, and e_0 is the sea-level vapor pressure, in centimeters. For an altitude h equal to the height of the limits of the atmosphere the equation reduces to

$$Q_2 = 2.3e_0. \tag{7}$$

If we substitute for h the altitude of the University of New Mexico and subtract (6) and (7) we will get an expression for the quantity of water above station D to the limit of the atmosphere.

[8] Hann, Lehrbuch der Meteorologie, p. 230; 1915.

$$Q = Q_2 - Q_1 = 2.3e_0 - 2.3e_0(1 - 10^{-1556/5000})$$
$$Q = 1.17e_0.$$

From Hann's relation between sea-level vapor pressure, e_0 and the vapor pressure at an altitude h, e_w, we get

$$e_w = e_0 10^{-1556/6500}$$
$$e_0 = 1.73e_w.$$

Substituting this value for e_0 in the equation for q we have

$$Q = 1.93e_w.$$

This gives the quantity of water in the vertical column of air above station D in terms of the observed vapor pressure. Thus at noon October 17, 1932 the vapor pressure was observed as 0.557 cm and Q was 1.08 cm.

In a similar way Q was determined for the other stations.

Station A—elevation 3140 meters—$Q = 1.64\ e_w$
Station B—elevation 2059 meters—$Q = 1.85\ e_w$
Station C—elevation 1769 meters—$Q = 1.87\ e_w$.

Formula (5) is written for unit air mass and the Q which is the amount of water above the observation point must be multiplied by B_0/B to give the q needed for formula (5). On the days on which observations were taken the vapor pressures at station D ranged between 0.13 to 0.61 cm and the corresponding values of Q from 0.5 to 1.4 cm.

Eq. (5) may be written in logarithmic form as $\log a = \log a_a + q \log a_w$. If now $\log a$ be plotted against q, the points should fall on a straight line which may be extrapolated to zero water to give the value of $\log a_a$. Fig. 3 shows such straight lines for the observations at 1556 and 2059 m. The values of the absorption coefficient so obtained are:*

at 3140 m $a = 0.47$	at 1769 m $a = 0.46$
at 2059 m $a = 0.47$	at 1556 m $a = 0.43$.

For the three higher elevations there is very good agreement in the values of "a". The coefficient observed at 1556 m shows the influence of dust and smoke of the nearby city which has caused about 10 percent decrease in transmission.

The scattering of the points about the line in Figs. 2 and 3 represents an uncertainty of about 5 percent. Partly this is due to inherent difficulties in outdoor observations under atmospheric conditions which cannot

* In the following pages of this article a will be written for a_a.

be controlled; in part the scattering is due to errors in the use of Hann's formula to calculate the amount of water in the path. These uncertainties are certainly not more than is usual and unavoidable in such observations and do not leave the final value of "a" in doubt by more than 4 or 5 percent.

The values of "a" at the higher elevations, which have been corrected for water vapour and which are only slightly, if at all, influenced by haze and dust, should be directly comparable with e^{-KX} of Rayleigh's formula. The only constant in doubt in $K=32\pi^3(\mu-1)^2/3N\lambda^4$ is λ.

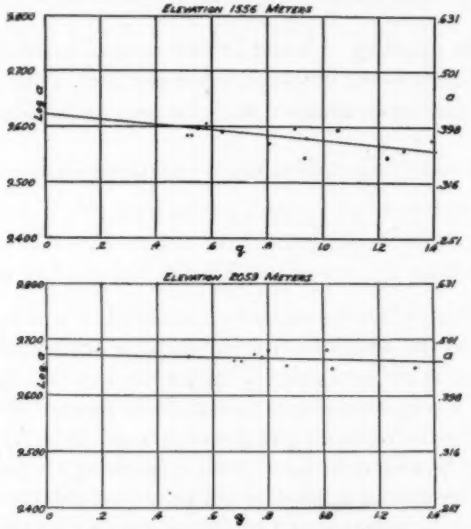

FIG. 3. *Transmissibility of radiation through moist air.*

Pettit[7] in his work with the solar radiation transmitted by a silver film used $\lambda 3200$ in computing K. It is true that $\lambda 3200$ is the center of the transmission band of silver.[9] However, the solar energy curve falls off very rapidly in this region and the wave length of maximum energy transmitted by the silver filter must be greater than $\lambda 3200$. The position of this maximum may be determined by plotting for each wave length the product, C, of the transmission of silver for that wave length by the relative energy of the solar spectrum, as is done in Fig. 4. The solar energy curve, A, is taken from measurements by Brian O'Brien, published by Forsythe and Christison[10] and the silver transmission, B, from

[9] Hagen and Rubens. Ann. d. Physik, *8*, p. 432; 1902.

[10] Forsythe and Christison, G. E. Rev., *32*, p. 662, 1929.

Hagen and Rubens.[9] It is seen that the wave length of maximum energy transmission is about λ3240. We have accordingly used that value in computing K. For this wave length $(\mu-1)=2.88\times10^{-4}$,[11] N is taken as 2.707×10^{19},[12] and X as 7.99×10^{5}.[13] With these values $e^{-KX}=a=0.479$.

In Table 2 are collected for comparison our values of "a" at the different elevations together with those reported by Pettit, which have been corrected to unit air mass. It will be noted that Pettit's value for "a" at Mt. Whitney is in almost perfect agreement with the calculated value.

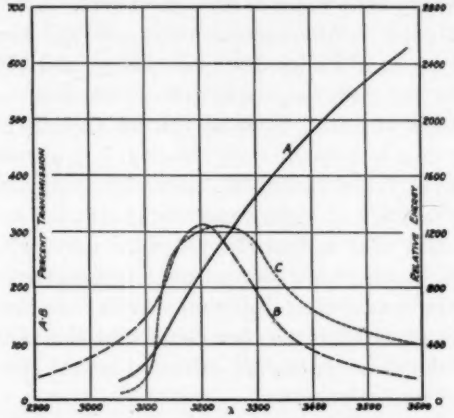

FIG. 4. *Maximum solar energy transmitted by silver near 3200. A, solar energy curve; B, transmission curve for silver; C, transmitted energy.*

TABLE 2. *Results in comparison. Rayleigh scattering by unit air mass.*

$a=e^{-kx}$ $\qquad$ $\mu-1=2.88\times10^{-4}$

$k=32\pi^3(\mu-1)^2/3N\lambda^4$ $\qquad$ $N=2.707\times10^{19}$

$\lambda=3.24\times10^{-5}$

$\chi=7.99\times10^{5}$

$a=0.479$ "a" for unit air mass

Observed at Albuquerque		Given by Pettit		
elevation	"a"	elevation		"a"
3140 meters	0.47	Mt. Whitney	3500 meters	0.475
2059 meters	0.47	Mt. Wilson	1740 meters	0.405
1769 meters	0.46	Tucson	760 meters	0.338
1556 meters	0.43	Pasadena	258 meters	0.320
		Oxford, Eng.	64 meters	0.312

[11] Smithsonian Physical Tables, 7th edition, p. 293; (1923).

[12] Birge, Phys. Rev. Sup. *1*, p. 1; 1929.

[13] Kimball, Monthly Weather Review *55*, p. 155; 1927.

Pettit himself used in calculation of "a", λ3200, as well as different values of the other constants, and obtained for a, 0.448. As pointed out above it seems to us that the effective wave length should be λ3240. Pettit's coefficients at elevations lower than Mt. Whitney are all smaller than would be expected from the formula. This may be accounted for by the fact that there is no evidence that there was any correction applied for the water vapor in the atmosphere. For the Mt. Whitney observations that fact would have little effect, since above an altitude of 3500 m there is very little water in the atmosphere.

In the work done at Albuquerque the agreement between the observed coefficients at altitudes 3140 m, 2059 m and 1769 m and the calculated molecular scattering coefficient is well within the error of observation. The low observed value at 1556 m altitude is undoubtedly due to effect of dust and smoke from the city. It is our intention to extend this work to lower elevations, and with improved methods of determining the amount of water vapor in the air path at low altitudes.

Our results show that at least for altitudes above 1700 m, and for clean dry air, the Rayleigh law for pure molecular scattering is adequate to account for the atmospheric depletion of solar radiation in the transmission band of silver. It is also our belief that this is the case at all altitudes when the observations are corrected for the effects of scattering by dust and water vapor.

THE EFFECT OF INTENSITY AND UNDERLYING FOGS ON THE LATENT IMAGE

By Franklin E. Poindexter and Louis E. James
[St. Louis University, St. Louis, Missouri. Received May 6, 1932]

Introduction

We are proceeding on the assumption that the formation of the latent image is a direct primary photomechanical process.[1] The action of the light on the silver halide crystal is thought to be that of cracking or shattering the crystal lattice along lines of strain. A grain becomes developable when sufficiently cracked and reversed or rendered developable when cracked too much due to the closing up of the cracks upon the relief of the strains.

This hypothesis is in agreement with many photographic phenomena. One of the outstanding difficulties in theories is that of the energy necessary in the formation of the latent image. In the first sentences of a recent paper by Sheppard,[2] we find: "In the course of their researches, Hurter and Driffield touched upon the formation of the latent image. With characteristic insight, they devoted their attention to the question of the amount of energy required. Using thermochemical data at their disposal, they concluded that the light could supply an extremely minute proportion only of the energy required to produce the final developed silver image." On a strain hypothesis, we might have an abundance of energy stored as potential energy of strain so that the light would pull the trigger, as it were, by inducing vibrations in the strained portions of the lattice, thus promoting and developing cracks. Consequently, a cracking-up hypothesis takes care of the question of the energy necessary for latent image formation.

Another experiment that confounds our present theories is that by Warnercke[3] of writing on a photographic film by means of a rounded glass stylus. Although the surface of the film was not scratched, the writing developed out black. This phenomenon is simply explained on a crystal-cracking hypothesis. The drawing of the stylus over the film cracks the surface crystals.

We could use much space with similar examples, but let us now return to the difficult phenomena of reversal. It is an experimental fact

[1] S. E. Sheppard and W. Vanselow, Jour. of Phys. Chem. *33*, pp. 250–273; 1929, especially noteworthy references are given on pp. 261–263.

[2] S. E. Sheppard, Photog. Jour. *68*, pp. 397–414; 1928.

[3] Warnercke, Phot. Archiv. p. 120; 1881.

that the density is directly proportional to the exposure in the early stages of the latent image formation, as shown in Fig. 3 below. Following this is a region wherein the density is directly proportional to the logarithm of the exposure. Later comes a region in which the density climbs *even slower*, till we reach the so-called region of first reversal in which the density is actually decreased by further exposure. If we continue the exposure, however, the graph will climb again and finally reach the region of second reversal in which the density is again falling with increasing exposure. These phenomena have put us to much trouble and, so far, we have not been able to make assumptions that will show our way out. This is a clear indication that our underlying physical concepts of the process are at fault.

Now it seems to us that the cracking-up hypothesis of latent image formation may serve as a basis for a theory which can include reversal as well as many other phenomena of photography. We regard any region of strain as a potential crack. It can hardly be questioned that the molecules in a region of strain will have a freedom of vibration that is different from those in an unstrained crystal. It is certainly well known that the absorption of light sets the molecules of a solid, liquid or gas into vibration. It is also well known that light will tear parts of various metals off, forming colloidal solutions.[4] We feel that we are taking a short step further when we say that under the influence of light a fissure may develop in a strained silver halide crystal.

It seems well established that development of a latent image starts about so-called sensitivity centers upon the surface of the silver halide crystals.[5] Whether these centers consist of occluded colloidal silver or of silver sulphide, they would be expected to cause strains in the crystal. Consequently, the cracking up process can well be expected to start around these centers. There would probably be a haphazard distribution of these cracks about a center. When a crack reaches a certain stage of growth it would render the halide grain developable. In case the crack growth is extended beyond certain limits we might expect a rearrangement or closing up and we have reversal predominating in the situation. Further exposure, however, causes a new crop of cracks in other grains to reach developability, till we reach the second stage of reversal. In this manner we at least get some sort of a physical basis for reversal.

Let us quote (p. 261) from the paper by Sheppard and Vanselow re-

[4] The Snedberg, Kolloid Zeits., *17*, p. 51; 1915; *21*, pp. 28–154; 1917.

[5] S. E. Sheppard and A. P. H. Trivelli, Photog. Jour. *66*, pp. 505–513; 1926.

ferred to above: "Many examples have been cited to demonstrate a direct mechanical disintegration by light acting on solids. Bredig and Premsel[6] suggested that the developable latent image was due to a photomechanical disintegration of the silver halide crystals. Actual disintegration can be observed in the case of silver iodide, as first noticed by C. Schultz-Sellack[7] and studied more fully by H. Scholl.[8] A very thin continuous layer of silver iodide is obtained by exposing a silver mirror to iodine vapor, this becomes turbid and varicolored by exposure to intense light and can be shown by rubbing to be actually mechanically disintegrated."

In a recent paper[9] from these laboratories it was shown that the application of pressure prevents the formation of the latent image to a great extent. Up to the time of this experiment it was generally believed that the application of pressure to a region of a photographic plate would cause that region to develop out black. It seems easy to account for this experimental result on a crystal-cracking hypothesis. That is, the pressure prevents the vibrational response of the molecules to the radiation. As a matter of fact, the pressures that were applied in this experiment rendered ordinary photographic paper as transparent as glass.

In the work to be described below, we have found that other, more detailed predictions of the hypothesis have been verified. Take, for example, the failure of the reciprocity law.[10] Aside from any hair-splitting calculations, if the formation of the latent image consists in a splitting up of the halide crystals due to damped resonant vibrations, we might well expect the violence of this cracking to increase faster than the increase in the intensity up to some optimum intensity. This would give two kinds of reciprocity law failure. That is, very low-intensity radiation would only develop cracks in the greatly strained regions of a few crystals giving us the Channon effect[11] of low maximum density which cannot be increased by increasing the time of exposure and, also, giving us small slopes of the ρ *vs.* log E graphs. It requires different times in which to bring different cracks up to developability; however, the radiation must be able to start a crack before it can carry it on to developability. Therefore, as we increase the intensity of the radiation we not

[6] Arch. Wiss. Phot. *1*, p. 33; 1899.

[7] Pogg. Am. *143*, p. 442; 1871.

[8] Ann. d. Physik *16*, p. 193, 417; 1905.

[9] F. E. Poindexter, J. Opt. Soc. *21*, pp. 59–69; 1931.

[10] A good bibliography on this phase of photography is to be found in a paper by E. A. Baker; Proc. Ray Soc. Edinburgh, *45*, pp. 166–186; 1924–1925.

[11] H. H. Channon, Photog. Jour. *45*, p. 164; 1920.

only produce the cracks with more speed and violence, but more cracks are now available to the radiation. This leads us to expect that the failure of the reciprocity law will be greater for low intensities than for high intensities up to the point where the using up of the strained crystals and reversal take charge of the situation. This is borne out by experiment. The straight line graphs of ρ *vs.* t, Fig. 3, serve to illustrate this point. Another illustration is the increase in the value of the Schwarzchild constant p, with intensity.

There are two more of our experimental results which seem to fit in with such an hypothesis. These are, first, a weak radiation is found to produce more blackening on a dense underlying fog than the reverse and, second, white light climbs to higher densities upon an underlying red fog than the red on the white. In the case of the intense and weak white light, we can hardly expect the reversal to be a straight line function of the intensity. If reversal is caused by the development of interlacing cracks to the extent that the crystal parts can reunite in a more or less unstrained condition, then we can expect the percentage of reversal of affected grains to be greater for intense light, since the greater violence of explosion would give greater and deeper lateral shatterings. When we have two sources of equal actinic value, but of different spectral width, such as white light and the red that we used, we would expect the white to produce a greater blackening on top of the red fog than the red on the white fog because the white radiation would be able to develop a greater number of the latteral cracks and strains due to its heterogeneous composition. That is, in any event when a crystal is cracking under the influence of a radiation there are secondary cracks and new strains produced in addition to the principal cracks. The greater the spectral width of the subsequent radiation the larger the number of cracks and strains subject to its influence.

Finally we have obtained a result which may or may not fit in so well with a photomechanical hypothesis. That is, we find that a weak, monochromatic radiation does not climb better on a strong underlying fog of the same radiation than the intense radiation on the underlying fog of the weak illumination. There must be a secondary cracking process in this instance too, but it may be that the secondary cracks are not susceptible to the narrow spectral width of the radiation.

EXPERIMENTAL

The exposures were made in a camera 12 ft.$\times$1 ft.$\times$1 ft. as shown diagrammatically in Fig. 1. This camera is so diaphragmed that no light

from the walls can reach the photographic plate. The openings in the diaphragms are bordered with the black paper used by the manufacturer for wrapping the plates.

Tungsten lamps, rated at 110 volts, were burned at 108 volts in front of the camera and so positioned that the emulsion was not exposed to the direct light of the filament. The lower diagram Fig. 1 shows the set-up for all white and all green light. The front of the camera is closed with a brass plate through which two thimbles project carrying ground glass plates on the inside ends. Each thimble served as a source of light when illuminated. The intensities were varied by introducing into the thimbles doubly ground glass disks cut from cleaned photographic plates.

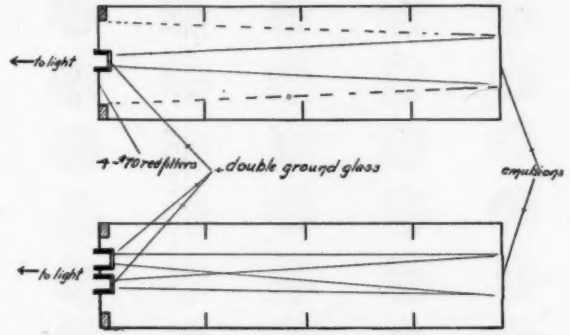

FIG. 1 *General arrangement of apparatus. Top, red-white; bottom, all-white. (Not drawn to scale.)*

A Copper-Hewitt mercury lamp was used in connection with corning filters G555Q and G34Y for the green light source. This gave us very approximately monochromatic light of 5461A.

In the case of the red and white and all red exposures, the upper diagram of Fig. 1 shows the arrangement. The front of the camera is closed with four sheets of Wrattan #70 filters carrying a thimble in the center through which white light was passed. By covering all but the thimble we had white only and by plugging the thimble we had red light falling on the plate.

Hammer extra fast plates* were used in all cases. They were all developed at 65°F with brushing for[12] five minutes in the following developer: water 128 oz., hydroquinone 75 g, sodium sulphide 240 g,

* We wish to thank the Hammer Dry Plate Co. of this city for the plates and for their hearty cooperation.

[12] W. Clark, Photog. Jour. p. 76; Feb., 1925.

sulphuric acid 3.5 cc, sodium carbonate 60 g, potassium carborate 180 g, potassium bromide 15 g.

DATA AND RESULTS

The data and results are displayed graphically. In Fig. 2, we have shown one of the plates ready for the photometer[13] upon which we meas-

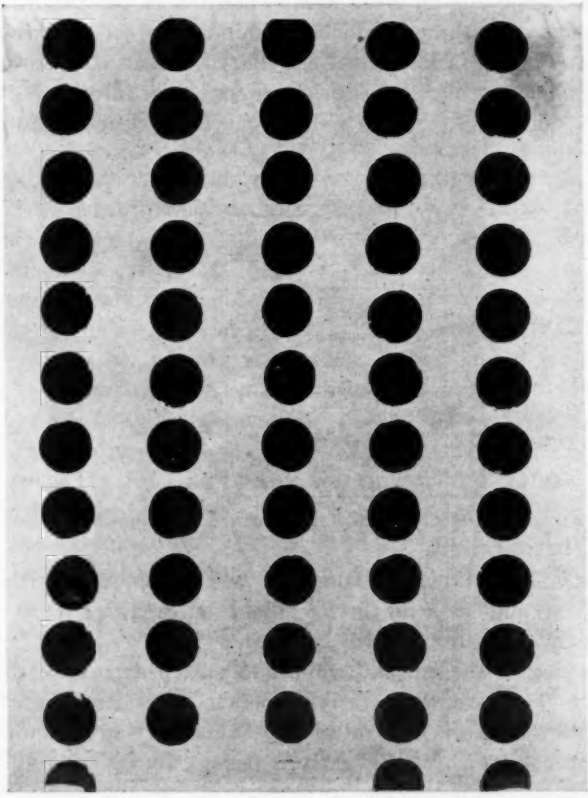

FIG. 2. *A reproduction of one of the plates.*

ured the diffuse density. These spots were exposed by pulling out strips so as to uncover successive holes in front of the emulsion.

Fig. 3 is obtained from plate No. 25, which was exposed to white light, by plotting the diffuse density against the time, t, in minutes This is

[13] F. K. Richtmyer, Phys. Rev. *6*, pp. 66–68; 1915.

done to show how remarkably straight these graphs are for low intensities. It will be noticed too, that the graphs are not parallel as we have become accustomed to for straight line ρ *vs*, log E graphs.

The two "on tops" and the "mixed" in Fig. 3 and in all the graphs following would have to be shifted to the right by a factor of 2 in order to display them on a true H and D scale, that is, the graphs marked 1 and 2, Fig. 3, show the density against the time for the two sources. The 2 on 1 and the 1 on 2 graphs, however, are plotted against only half of

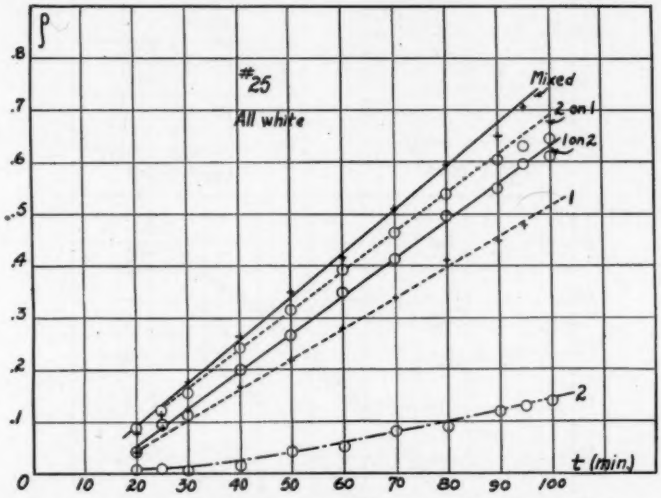

FIG. 3. *A graph of plate No. 25 showing the linearity of the density against time at low intensities.*

the total time since each was placed on top of an equal time fog of the other source. The highest graphs, marked mixed, show the density against the time of exposure for both sources shining simultaneously. In this manner, any given ordinate cuts the three upper graphs at points of equal exposure, where exposure is understood to mean the product of the intensity times the time of exposure. In other words, the same amount of light energy fell upon the photographic plate for each of the three upper points on a common ordinate. The two underlying curves are to be compared with each other showing the relative actinic values of the sources. This was a convenience for us and saves confusion, since in many cases the single source graphs would overlap the on tops and the mixed, if they were all plotted as ρ *vs*. log E graphs.

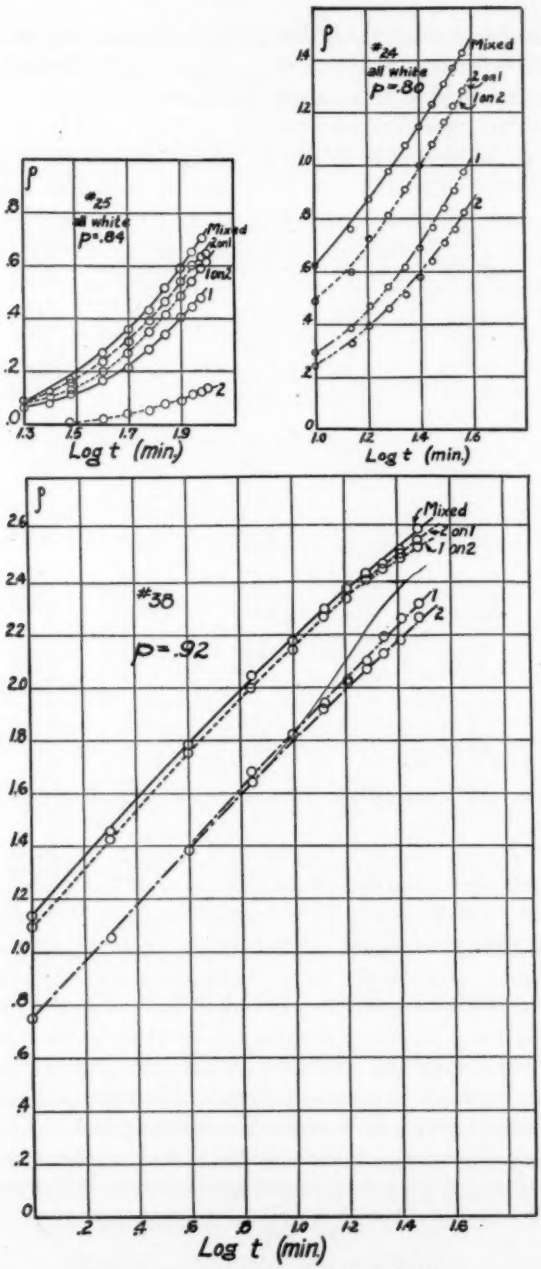

FIGS. 4, 5, AND 6. *Graphs for white light plates.*

Figs. 4, 5 and 6 are ρ *vs.* log t graphs for all white light exposures. Fig. 4 is for the same plate as was used for the graphs in Fig. 3. It will be noticed that the mixed or combined intensity graphs are higher than the on tops in all cases, showing that the reciprocity law does not hold even at the higher intensities used in plate No. 38. The remarkable

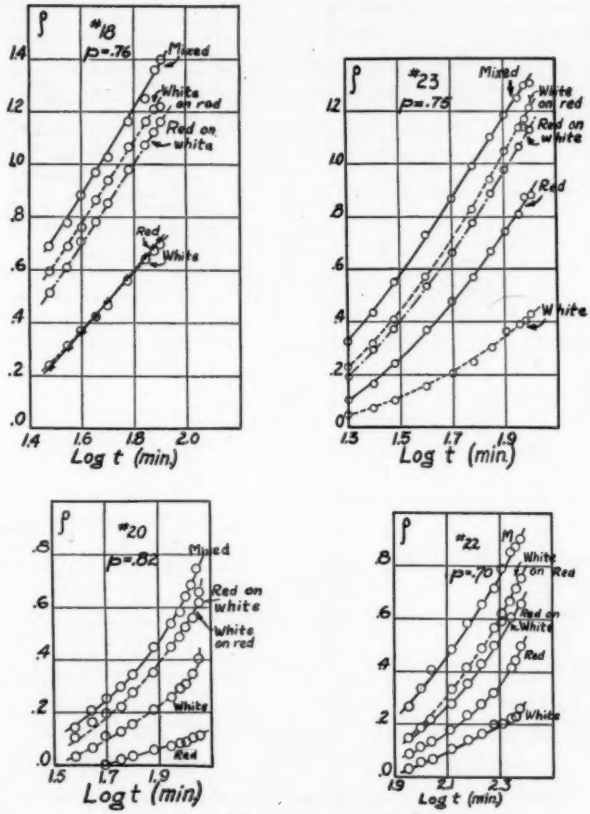

FIGS. 7, 8, 9 AND 10. *Graphs for white and red lights.*

point, however, is the fact displayed in plate No. 25, that a weak radiation No. 2 on top of the strong underlying fog of No. 1 gave higher densities than the opposite arrangement.

The ρ *vs.* log t graphs for the red and white light combinations are shown in Figs. 7, 8, 9 and 10. The two colors are of approximately equal actinic values in Fig. 7 and of unequal actinic values in the other three

plates. When the white light is equal to or less than the red in actinic value, it is more efficient photographically on the underlying fog of the red light than is the red on the white. In Fig. 9, however, the red is so much weaker than the white, that its advantage in this respect balances the better climbing abilities of the white, and the on tops come together.

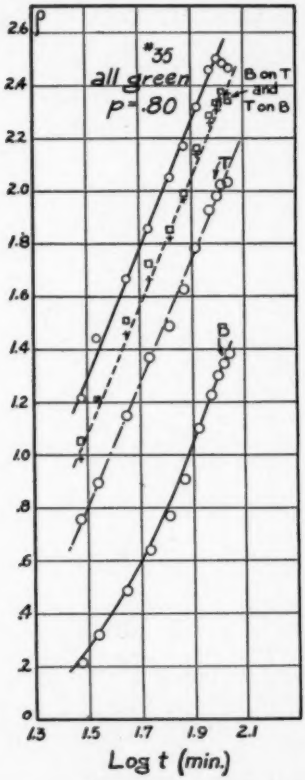

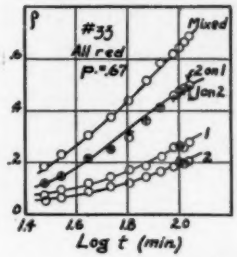

FIG. 11. *Graph for red light.*

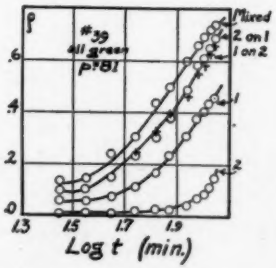

FIGS. 12 AND 13. *Graphs for green light of wave length 5461A.*

The ρ *vs.* log t graphs for the monochromatic radiations of red light and of green light are shown in Figs. 11, 12 and 13. It will be observed that in all these plates the on tops come approximately together regardless of differences in the intensities of the two sources.

The deviation from unity of the Scharzchild exponent in the equation $\rho = \log It^{\gamma}$ where ρ is the density, I is the intensity and t is the time of exposure, can be thought of as a measure of the reciprocity law failure.

The values of P given on the graphs were calculated by means of the relation.[14] $S = [(1-p)/p] \log I_1/I_2$ where S is the mean horizontal displacement of on tops graphs from the mixed for a given ρ. The intensity for the on top graphs was taken as the arithmetical mean of the two intensities while that for the mixed was taken as the sum, so that log I_1/I_2 becomes log 2.

Since the question of decay and growth of the latent image in the interval between exposure and development has occupied the attention of a number of workers,[15] it was thought worth while to make a series of

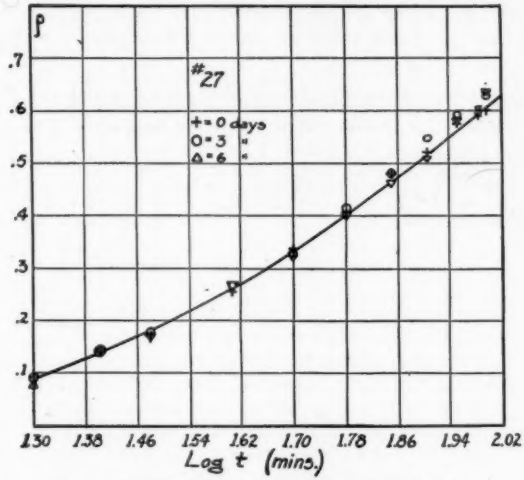

FIG. 14. *Graph showing the absence of rest-period effects.*

exposures at intervals of several days on the same plate and then to develop immediately after the last exposure. Fig. 14 shows the results of such an experiment. These results are completely negative, showing that we do not have a rest period factor in our plates.

Each of the graphs presented in this paper has been selected from several that bring out the point illustrated. In no plate have we obtained negative results, or results differing widely from those presented. Since there is such a wide divergence between the densities and even between the slopes of ρ—*vs*—log E graphs of plates of the same emulsion under identical conditions of exposure and developing, we feel that it is better

[14] *Physics of the Developed Photographic Image*, by F. E. Ross, p. 67, Eastman Kodak Co., Rochester, N. Y., 1924.

[15] P. C. Keenan, Astrophys. J. *74*, pp. 105–109; 1931.

to display the data for each plate separately than to attempt a process of averaging. The errors in our density measurements are well within 1 percent.

SUMMARY

1. We have found that there is a considerable deviation from the reciprocity law for fast plates and that this failure is greater for low intensities.

2. We find that a white radiation of low intensity is more efficient when placed on the latent image of a stronger light than when the order of exposure for the two lights is reversed.

3. White light is more efficient on an underlying red fog than the reverse.

4. Both green and red light of narrow spectral width fail to show any appreciable difference in the efficiency with intensity as was found in the case of the white light.

5. We feel that our results support a crystal shattering hypothesis of latent image formation.

THE FUNCTION OF sin x/x

By Simon H. Bauer

[Jones Chemical Laboratory, University of Chicago, Chicago, Illinois. Received February 18, 1932]

Due to the fact that considerable work must be expended to obtain values of sin x/x, a function particularly useful in calculations of diffraction phenomena, it was thought advisable to publish the table compiled in this laboratory as an aid to other investigators.[1] The values given below have been checked by a large scale plot, all points having been found to fall on a perfectly smooth curve. Values of x are in radians.

x	sin x/x	x	sin x/x	x	sin x/x	x	sin x/x	x	sin x/x
0.00	1.00000	0.5	+0.95884	13.0	+0.03232	25.5	+0.01404	38.0	+0.00780
0.1	0.99830	1.0	+0.84146	13.5	+0.05954	26.0	+0.02933	38.5	+0.01865
0.2	0.99335	1.5	+0.66499	14.0	+0.07076	26.5	+0.03696	39.0	+0.02471
0.3	0.98506	2.0	+0.45464	14.5	+0.06447	27.0	+0.03542	39.5	+0.02465
0.4	0.97355	2.5	+0.23938	15.0	+0.04335	27.5	+0.02542	40.0	+0.01862
0.5	0.95884	3.0	+0.04704	15.5	+0.01332	28.0	+0.00967	40.5	+0.00825
0.6	0.94107	3.5	−0.10022	16.0	−0.01800	28.5	−0.00785	41.0	−0.00387
0.7	0.92030	4.0	−0.19920	16.5	−0.04314	29.0	−0.02289	41.5	−0.01476
0.8	0.89670	4.5	−0.21723	17.0	−0.05655	29.5	−0.03190	42.0	−0.02182
0.9	0.87035	5.0	−0.19178	17.5	−0.05575	30.0	−0.03293	42.5	−0.02344
1.0	0.84146	5.5	−0.12828	18.0	−0.04172	30.5	−0.02600	43.0	−0.01934
1.1	0.81019	6.0	−0.04656	18.5	−0.01851	31.0	−0.01303	43.5	−0.01066
1.2	0.77670	6.5	+0.03310	19.0	+0.00783	31.5	+0.00267	44.0	+0.00041
1.3	0.74121	7.0	+0.09386	19.5	+0.03106	32.0	+0.01724	44.5	+0.01112
1.4	0.70389	7.5	+0.12493	20.0	+0.04565	32.5	+0.02720	45.0	+0.01891
1.5	0.66499	8.0	+0.12367	20.5	+0.04863	33.0	+0.03030	45.5	+0.02195
$\pi/2$	0.63662	8.5	+0.09394	21.0	+0.03984	33.5	+0.02600	46.0	+0.01960
1.6	0.62473	9.0	+0.04578	21.5	+0.02193	34.0	+0.01556	46.5	+0.01256
		9.5	−0.00792	22.0	−0.00041	34.5	+0.00166	47.0	+0.00263
		10.0	−0.05440	22.5	−0.02166	35.0	−0.01224	47.5	−0.00774
		10.5	−0.08378	23.0	−0.03679	35.5	−0.02279	48.0	−0.01601
		11.0	−0.09091	23.5	−0.04247	36.0	−0.02755	48.5	−0.02023
		11.5	−0.07612	24.0	−0.03773	36.5	−0.02552	49.0	−0.01925
		12.0	−0.04471	24.5	−0.02413	37.0	−0.01739	49.5	−0.01400
		12.5	−0.00530	25.0	−0.00529	37.5	−0.00527	50.0	−0.00524

[1] G. Bruhat, *Cours D'Optique*, p. 216 gives a table of values of sin x/x which runs from 0 to $4\pi/12$ in steps of $\pi/12$.

Keiichi Hayashi, *Tables of Bessel, Theta, Spherical and Other Functions*, presents a table of sin x/x values in which the argument varies from 0 to 15.9 in steps of 0.01.

CORRESPONDING RETINAL POINTS, THE HOROPTER AND SIZE AND SHAPE OF OCULAR IMAGES*

By A. Ames, Jr., Kenneth N. Ogle and Gordon H. Gliddon
[Department of Research in Physiological Optics, Dartmouth Medical School, Hanover, New Hampshire. Received June 2, 1932]

TABLE OF CONTENTS

PART I

Page

I. Preface 538
II. Introduction 539
A. NATURE OF CORRESPONDING POINTS 539
B. OPTICAL PROJECTION OF CORRESPONDING RETINAL POINTS. 541
C. PROJECTION FANS, SIZE AND SHAPE OF OCULAR IMAGES AND THE HOROPTER 545
D. CORRESPONDING FUSIONAL AREAS 550
III. Description of Apparatus 554
A. APPARATUS FOR HOROPTER DETERMINATIONS AT NEAR 555
B. APPARATUS FOR HOROPTER DETERMINATIONS AT A DISTANCE 561
IV. Experimental Procedure 564
V. Method of Analyzing Empirical Data 566

I. Preface

This laboratory has been interested of late primarily in the physiological and clinical significance of the relative size and shape of the ocular images of the two eyes.[1] Since the relative size and shape of ocular images and the problem of corresponding retinal points are closely related, a thorough understanding of the latter became most important. Although considerable work has been done on the study of the correspondence of retinal points and the horopter, much remains to be determined. The following paper describes a series of studies which was undertaken in the laboratory to obtain further knowledge of the subject. From the point of view of evolutionary sequence this work follows the study and researches of Tschermak and his associates.[2] If advance has

* Acknowledgment is made to an anonymous donor for a subvention partially to defray cost of publication of this article. Editor.

[1] *Ocular Measurements*, Trans. Sect. on Ophthalm. of A.M.A.; 1928. *Size and Shape of Ocular Images. I. Methods of Determination and Physiologic Significance*, Arch. of Ophthalm. *7*, pp. 576–597; 1932. *II. Clinical Significance*, Arch. of Ophthalm. *7*, pp. 720–738; 1932. *III. Visual Sensitivity to Differences in the Relative Size of the Ocular Images of the Two Eyes*, Arch. of Ophthalm. *7*, pp. 904–924; 1932.

[2] Optischer Raumsinn, Bethes Handbuch der Normalen u. Pathologischen Physiologie *12*, Part 2, pp. 834–1000; 1930.

been made it is due to the foundation which they laid and upon which this work is based.

In general the paper will present, first, a general introduction to the problem of the correspondence of the ocular images; second, criteria and methods of determination; third, changes that take place with variations in phoria, fixation distances and with asymmetrical convergence of the eyes; fourth, the effects resulting from changing the size and shape of the dioptric images of the eyes by means of lenses.

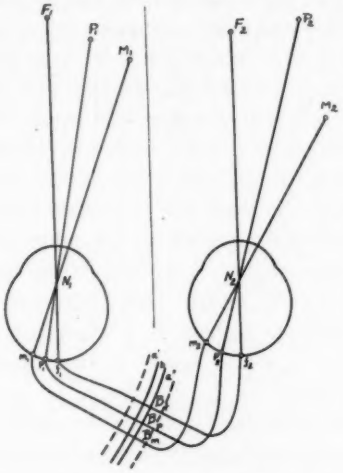

FIG. 1. *Schematic representation of the cortical connections and the optical projections of corresponding retinal points.*

II. INTRODUCTION

A. THE NATURE OF CORRESPONDING RETINAL POINTS

The factors which must be grasped for an understanding of the phenomena of correspondence of ocular images* and the horopter, are somewhat complicated and involved. An attempt will be made to give a condensed presentation of the subject. The whole matter is based on the anatomical structure of the oculo-sensory nervous system. Every point on the retina of one eye has a primary nerve connection to a specific

* The term ocular image is used here to describe the impression formed in the higher brain centers through the vision of one eye. It is determined not only by the properties of the dioptric image that is formed on the retina of the eye, but also by the modifications imposed upon it by the anatomical properties and physiological processes by which this optical image is carried to the higher brain centers.

brain center to which a specific retinal point in the other eye is similarly connected. In Fig. 1, let f_1 and f_2 represent elements on the retinas of the two eyes that are connected to a common center B_f in the brain.[3] Such retinal points are said to be "corresponding" since they function through the same brain centers. If a particular center in the visual cortex is excited a subjective impression of a particular direction relative to an egocentric center will be experienced.[2] The same subjective impression will be experienced whether the excitation of the particular brain center is caused by a stimulation coming from one eye or the other. Thus, schematically, in Fig. 1, the same subjective impression of direction will result whether the specific brain point B_f is excited by stimulations coming from either f_1 or f_2. If another brain center is excited, a subjective impression of a different direction will result. If two brain centers are excited at the same time, the impression of the two subjective directions will result. These two directions will have a definite and a particular relationship one to the other and will give a subjective impression of a particular directional separation. Schematically, if brain centers B_p and B_f in Fig. 1 are excited, a subjective impression of a particular directional separation will result. This separation will be the same whether the brain centers B_p and B_f are excited by stimulating the retinal points P_1 and f_1 in one eye or P_2 and f_2, their corresponding retinal points in the other.

If brain centers more widely separated as $B_m B_f$ are excited, say by stimulating retinal points which have a greater separation, a subjective impression of greater separation or size will result; likewise if brain centers less separated are excited, the impression will be of lesser separation or size. If three brain centers are excited, subjective impressions

[3] A satisfactory description of the neurological arrangement was given by Verhoeff. He states the theory that "there is a separate cortical system for each eye [see a', a'', Fig. 1] and that connecting the two systems and bringing them into relation with one another there is a third system, [see b Fig. 1] composed of a more or less complicated arrangement of neurones, upon which the binocular perception of relief is dependent. This intermediate system may thus be regarded as the cerebral representative of the hypothetical cyclopean eye of Hering and others, and may be spoken of as the cyclopean center, and with it all ideas concerned with binocular relief would be associated It is further assumed that the monocular systems may act independently both as regards each other and as regards the cyclopean center." (A Theory of Binocular Perspective etc., p. 11, Ann. Ophth., Apr. 1902.) Since Dr. Verhoeff advanced this conception of the ocular nervous system as a theory in 1902, knowledge regarding the anatomical relations of those portions of the brain concerned with vision has increased considerably and has not only confirmed the correctness of Verhoeff's theory but indicates that the cyclopean center is anatomically intermediate in position with relation to the monocular systems. Henschen, Arch. f. Ophthalm. *117*, pp. 403, 419; 1926. See also Lloyd Etiology of Strabismus, Archives of Ophthalmology 7, pp. 934–953; 1932.

of three directions and two space values result. These space values have a definite subjective relation to each other. For example in Fig. 1, the excitation of three brain centers B_f, B_p and B_m gives subjective impressions such that a quantitative differentiation can be made between the directional separations of B_fB_p and B_p and B_m. This holds true whether these brain centers are excited by impulses coming from one eye or the other.

Thus it will be seen that the stimulation of either one or both of a pair of corresponding retinal points excites the same brain center and produces one subjective directional value; that the stimulation of two

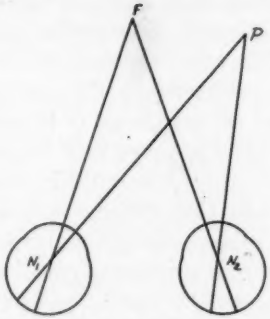

FIG. 2. *Schematic representation of the eyes in normal binocular vision.*

pairs of corresponding retinal points excites two brain centers and produces a definite subjective directional separation value while the stimulation of three pairs and hence three brain centers gives a subjective impression of two separations whose subjective magnitudes can be differentiated. It is on these relationships that the empirical determinations of retinal correspondence are based.

B. OPTICAL PROJECTION OF CORRESPONDING RETINAL POINTS

In general all empirical determinations made in the study of the phenomena of corresponding points consist in finding the position in space of pairs of objects that appear to have the same direction as seen by either eye. As illustrated in Fig. 1, such determinations consist in finding such positions of objects F_1, P_1, F_2 and P_2 in space, that F_1 seen by the O.S. appears in the same direction as F_2 seen by the O.D., and P_1 seen by the O.S. appears in the same direction as P_2 seen by the O.D. The objects may consist of two pairs, one pair being seen by each eye, or of one pair seen binocularly as shown in Fig. 2. The position of such

objects relative to the eyes is given by their distance from some optical or anatomical point in each eye, as the assumed mean nodal point or the apex of the cornea. The problem of obtaining information as to the correspondence of the ocular images from such determinations is not as simple as might at first appear. For instance, suppose pairs of objects which are imaged on corresponding retinal points in each eye have different separations, as in Fig. 1, where F_1P_1 and F_2P_2 are imaged on corresponding retinal points in each eye but the measurable angle between objects F_1P_1 before the O.S. is less than that between objects F_2P_2 before the O.D. This difference of angular separation indicates that the optical projections of the retinal points p_1f_1 in the O.S. subtend a lesser angle than do the optical projections of corresponding points p_2f_2 in the O.D. Difficulties arise in attempting to specify accurately the difference in the angles subtended by F_1P_1 and F_2P_2. In general every point on the retina may be considered to be projected outward along some path. The positions in space of such projection paths are determined by the particular nature of the optical system through which they are projected. In a complicated system, such as the eye, the paths of projected retinal points are a series of lines whose intersections lie on a caustic surface and not at a common point. The exact difference between the angles subtended by optical projections of corresponding retinal points cannot be determined without a knowledge of the exact positions of the points of intersection of these projections, which at present are unknown.

If the exact position of the paths of the optical projections of retinal points were known the problem would be simpler. Projection lines could then be drawn from pairs of objects having apparent equal separation, to the retina of each eye, and the relation between the separation of the optical projections of pairs of corresponding points accurately determined. For instance in Fig. 1 if the paths F_1f_1 and F_2f_2 and P_1p_1 and P_2p_2 could be drawn, the exact relative size of the angles $F_1N_1P_1$ and $F_2N_2P_2$ could be ascertained. These two angles representing the separation of projection lines from pairs of corresponding retinal points would give the relative effective distribution of corresponding retinal points. The difference between these angles, expressed in terms of percent would give the effective correspondence for those particular pairs of corresponding retinal points.

If the distance of the two retinas from N_1 and N_2 could also be determined, the exact position of corresponding points on the retinas could be ascertained.

Unfortunately the exact position of the paths of optical projection cannot be known.[4] The lack of this knowledge prevents the exact relative position of optical projections of corresponding points from being ascertained. However, in spite of the lack of such data very valuable and useful information can be obtained from the available determinations. By making certain assumptions as to the nature and position of the paths of optical projection, the relative position of the projections of corresponding points can be ascertained subject to a slight error, but an error so small in fact that it can be neglected for most purposes.

The assumptions that must be made are that the projection paths are straight lines and that they all pass through single mean nodal points at fixed distances from the cornea of each eye. Such assumptions

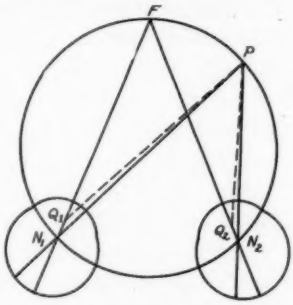

FIG. 3. *Schematic representation illustrating the error introduced by a misplacement of the assumed mean nodal points.*

introduce errors of two different natures. First, an error is introduced in assuming that all the projection paths cross at one point. In fact their intersections form a caustic and not a point. Second, an error is introduced in assuming the nodal points for all eyes to be at the same distance from the apex of the cornea. The error in the calculation of the relative separation of the projections of pairs of corresponding retinal points resulting ffom the above-mentioned assumption is small, for the reason that the distance from the eyes, of the objects, whose positions are determined, is very great compared to the possible errors in the positioning of the nodal point. This is made evident from a study of Fig. 3. Suppose the positions of P and F are determined relative to N_1 and N_2, which represent the actual position of the intersections of the

[4] Nor can the exact position of the retinas be known. Until both the exact position of the path of optical projections and also the position of the retina is known there is no hope of ascertaining the exact anatomical position of corresponding retinal points.

optical projections of pairs of corresponding retinal points. The relation between the projection of pairs of corresponding retinal points will be given by the angles $P\ N_1F$ and $P\ N_2F$ when P and F appear to each eye to have the same position and separation. In the particular case illustrated, P and F lie on the Vieth-Müller circle, and the angles $P\ N_1F$ and $P\ N_2F$ will be equal. Suppose now both mean nodal points are assumed to be at Q_1 and Q_2 in front of N_1 and N_2. The angles $P\ N_1F$ and $P\ N_2F$ become $P\ Q_1F$ and $P\ Q_2F$. Although the relation between the angles $P\ Q_1F$ and $P\ Q_2F$ is different from that between $P\ N_1F$ and $P\ N_2F$, the difference is very small. As can be seen from the figure, the magnitude of the difference in the relation of the angles resulting from misplacement of the nodal points, varies with the distance of the object F away from them. If the fixation object is at infinity it is zero, gradually increasing as the distance of F from the eyes is decreased. But even

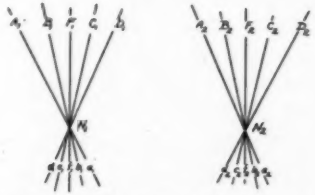

FIG. 4. *Schematic representation of the concept of projection fans to corresponding points.*

at near distances it is very small. Let it be assumed that for all cases all projection rays pass through a mean nodal point which lies about 7.30 mm behind the cornea. The intersection of any particular projection for any particular individual may vary from this average nodal point for three reasons. First, the particular individual may have eyes larger or smaller than the normal, in which case the distance of the nodal point from the cornea would differ from 7.30 mm. Second, the nodal point may be shifted, due to an accommodative change. Third, the ray in question may be quite oblique in which case the assumed mean nodal point would be in error.

A study of the variation due to the above causes shows first, that the distance of the mean nodal point from the cornea in the largest and smallest adult eyes probably does not vary by more than 2.0 mm; second, the movement of the nodal point resulting from an accommodative change from complete relaxation to a maximum accommodation is only about 0.5 mm; third, the calculated shift of the intersection of contiguous projection rays, having an obliquity of 20°, amounts to

about 1.1 mm. If all these variations were to take place at the same time, they would amount to a shift of about 3.0 mm. Now a misplacement of the nodal points of 3 mm introduces percentage changes in the difference of the angles, $P\ N_1F$ and $P\ N_2F$ when the latter is 16°, for various fixation distances as follows: of 0.006 percent at 100 cm, 0.037 percent at 40 cm and 0.15 percent at 20 cm. In view of the fact that the least perceptible difference in angular size of objects is around 0.15 percent to 0.25 percent these errors can be neglected for most purposes.

C. PROJECTION FANS, SIZE AND SHAPE OF OCULAR IMAGES AND THE HOROPTER

The angular relationship of the projection of pairs of corresponding retinal points is given subject to the negligible errors above mentioned, by the angles which are subtended at the nodal point of each eye by pairs of objects which appear to have the same direction as seen by either eye. By a similar method the angular relationship of the projections of a series of corresponding points across the retinas, can be determined. For example see Fig. 4. Separation F_1B_1 must appear equal to F_2B_2, F_1A_1 must appear equal to F_2A_2, etc. The relationship of the angles $F_1N_1B_1$ to $F_2N_2B_2$ and $F_1N_1A_1$ to $F_2N_2A_2$, etc., will give the relation between the projection of corresponding retinal points f_1b_1 and f_2b_2 and f_1a_1 and f_2a_2, etc.

Projection lines so determined give the position in space of the projection of corresponding retinal points. Their positions, however, do not give any information as to the relative subjective space or directional value associated with each particular pair of corresponding points as determined. That is, nothing has been determined as to the subjective spatial relationship that exists between the angles $F_1N_1B_1$ and $B_1N_1A_1$ or $F_2N_2B_2$ and $B_2N_2A_2$. For complete information it is necessary to know that the lines are projections of corresponding points and also to know the subjective directional value associated with each of the various projections. The directional value associated with a pair of corresponding retinal points is the value that is associated with the specific brain center to which they are connected. The directional values associated with a series of pairs of corresponding points are the series of values associated with the series of brain centers to which the corresponding points are connected. The most convenient directional values to characterize a series of projections of corresponding retinal points are those which cause the series of projections to appear equally spaced. Experimentally this is accomplished by positioning the objects that are im-

aged on corresponding points so that they all appear equally spaced.[5] With this information the relation of the projections of a series of corresponding retinal points in any one meridian, is determined and expressed in the relative disposition of the ribs or projection lines of the two fans which radiate from the mean nodal points.

Such fans give complete information concerning the relative size of the ocular images in the meridian in which they are determined. For example, if the fan of one eye is more extended than that of the other, that is, if greater angular separations exist between the corresponding projection lines, the same object in space will appear smaller when looked at with the first eye than with the other. This is because the image in the eye with the larger fan will stimulate retinal elements that

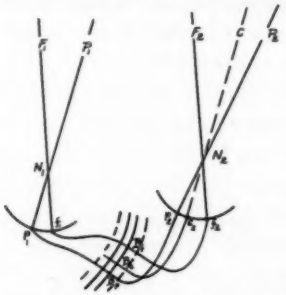

FIG. 5. *Schematic representation of the cortical connections and the optical projections of corresponding points when those of one eye are less separated than those of the other.*

are connected with the brain points that are less separated. This is apparent from a study of Fig. 5 where p_1p_2 and f_1f_2 are corresponding retinal points, and where the projection fan in the right eye is larger than that in the left eye. An object of the angular size of F_1P_1 before the right eye will form an image of the size of f_2c_2 in the right eye. This image in the right eye will excite brain points B_fB_c which have less extension than brain points B_pB_f and will therefore appear smaller.[6]

[5] It can also be done monocularly as will be explained later.

[6] This relationship between the apparent size of objects, the size of the image formed on the retina and the extent of the projection fans, tends to be somewhat confusing. If an object forms images on corresponding retinal points of both eyes it will appear the same size to both eyes and both projection fans will have the same extent. If a converging lens is put before one eye it causes a larger image to be formed on the retina. This larger image will excite brain centers that give a subjective impression of more extended space values and the object will appear larger as seen by that eye. The ocular image of that eye can be said to be larger. The effective projection of corresponding retinal points of that eye, however, will have less extent than it did before the lens was put before it for the reasons above stated. Another way of ex-

The shape of the image of each eye is also known if the projection fans are known. If the projection fan of one eye is more extended on one side and less so on the other, then objects to that eye will appear smaller on the side of the field of view where the fan is more extended and larger where it is not. The projection fans however do not give the absolute size of the ocular images. Both ocular images might be increased or decreased together but changes in size could not be determined from the fans.

From these projection fans the shape of the horopter can also be exactly determined. The relationship between the horopter and the projection fans can best be explained through some examples. The

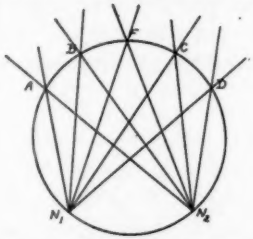

FIG. 6. *Illustration showing that the Vieth-Müller circle is the loci of the intersects of identical projection fans.*

simplest is shown in Fig. 4. F_1 and F_2 are the objects in space on which both eyes are fixated and the lines in the fans represent optical projections of corresponding retinal points. The arrangement of the projection lines in each fan as illustrated, is such that the corresponding projection lines all make equal angles with the fixation projection line, that is, $A_1N_1F_1 = A_2N_2F_2$ and $B_1N_1F_1 = B_2N_2F_2$, etc. The distribution of the projection lines in the two fans is identical and, if superimposed, the lines would coincide. That is, the lines in the fans subtend the same angles with the fixation line, and the fans are the same size. In such a case objects which subtend the same angle to each eye will appear to have the same directional separation or size as seen by each eye and will appear free from distortion.

If the eyes are used in binocular vision the fixation rays which are projected from corresponding retinal points at the centers of the foveas

plaining this is, that with the plus lens the nodal point of the combined optic systems of the lens and the dioptric system of the eye is moved forward. This is what causes the object to form a larger image on the retina. Also corresponding retinal points which of course have not changed their position, will, when projected through the advanced nodal point, form a less extended fan.

will intersect at the fixation point and there will be a general intersecting of the lines in the two fans. See Fig. 6. The points in space where corresponding lines in the two fans intersect is of special importance, for objects placed at such intersection points will be imaged on corresponding retinal points of the two retinas. It will be seen that the loci of all such points determine a line in the visual plane and that this line defines the trace of the longitudinal horopter since the horopter by definition is that surface in space every point on which is imaged on corresponding retinal points. With given projection fans never more than one horopter is possible. For the particular type of projection fans described, the horopter will lie on the so-called Vieth-Müller circle which passes through the fixation point and the mean nodal point of each eye.

For further illustration assume that the projection fans differ from each other in their extent and in the arrangement of their corresponding

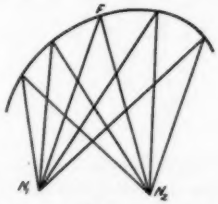

FIG. 7. *Illustration of the rotated position of the horopter trace when one of the projection fans has been extended overall.*

lines. Then the nature of the effective retinal correspondence will be different as will also be the horopter. For example, suppose the projection fans differ in that the lines in the O.D. fan are more separated by a constant amount overall than those of the O.S. Then objects which subtend the same angle to each eye will appear to be of different size. To the O.D. with its more extended fan they will appear smaller. The horopter will change slightly in shape and will be rotated, as shown in Fig. 7, as if about a vertical axis passing through the point of fixation. The direction of rotation of the temporal field will be away from the eye with the more extended fan. The projection fans may differ in that, while being of the same extent, the corresponding projection lines are asymmetrically spaced as shown in Fig. 8. Objects which subtend the same angle to each eye will appear to be the same overall size but distorted to each eye, the temporal sides of the object for each eye appearing smaller than the nasal. The trace of the horopter will take the form shown.

From the shape and position of the horopter it is also possible to determine to some extent the characteristics of the two fans. For instance, if the empirically determined horopter lies on the Vieth-Müller circle the fans must be of the same overall size or extent and their lines identically arranged. If the horopter is rotated about the point of fixation then the separation of adjacent lines of one fan must be greater than

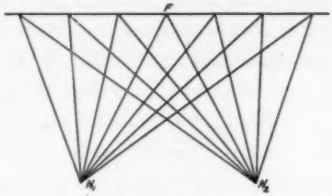

FIG. 8. *Illustration of the asymmetrical form of the projection fans whose intersects lie on the fixation frontal plane when those fans are equal.*

that of the other. If the horopter lies in the fixation frontal plane there must be a characteristic asymmetric distribution of the lines between the two fans. However, the shape of the horopter itself does not give as evident or as complete information as to retinal correspondence as does the distribution of the projection lines in the two fans. With the same shape horopter it is possible to have various distributions of the lines

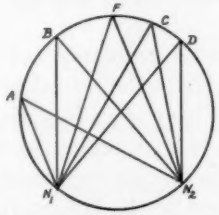

FIG. 9. *Illustration of the projection fans whose intersects lie on the Vieth-Müller circle, both of which are similarly asymmetric.*

in the projection fans. For instance, suppose the shape of the horopter trace is a straight line at all distances, then although it remains the same, the nature of the retinal correspondence must vary for the different distances. The nature of the correspondence can be calculated by taking the distance into account. The shape of the horopter alone does not give it. For example, assume a horopter has been determined as lying on the Vieth-Müller circle. With such a horopter the fans must be of the same overall extent and the corresponding projection lines must

form the same angles with the fixation lines, but it gives no information as to the relation of these lines to each other. It might be that the projection lines which make angles of equal apparent separation are much nearer together on the same sides of both fans, as shown in Figs. 9 and 10. The horopter in the first case would still be on the Vieth-Müller circle but that fact gives no information as to the relative size of the angles $F\ N_1\ B$ and $F\ N_1\ C$ or $F\ N_1\ A$ and $F\ N_1\ D$.

Similarly, when the horopter lies on the fixation frontal plane, the lines in the two fans must be asymmetrically distributed, but just what that distribution is cannot be ascertained from the shape of the horopter itself. To obtain information that will definitely determine the position of the lines in the fans, horopter determinations must be supplemented by another type of empirical determinations as Fischer and Tschermak have pointed out.

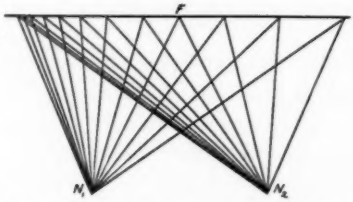

FIG. 10. *Illustration of the projection fans whose intersects lie in the fixation frontal plane, both of which are asymmetric in the same direction.*

It should be borne in mind, moreover, that under certain conditions intersects may not exist; that is, the optical projections of corresponding retinal points may never meet. This happens when one eye is turned away relative to the other, e.g., in squint. In marked cyclotropia, where one eye is rotated about its fixation axis relative to the other, there will be no such intersects except at the intersect of fixation, in which case the horopter exists only at a point in space. If there is fixation disparity in addition to cyclotropia, a horopter cannot exist even at the fixation intersect.

D. CORRESPONDING FUSIONAL AREAS

If the only connections between corresponding retinal points and the brain were the primary ones as described above, all objects in space that do not lie on the horopter would be seen double. This is, of course, not true, for not only are those objects that lie on the horopter seen singly but all objects that lie within a certain specific distance of the horopter are also seen singly. Thus, within certain limits objects which

are not imaged on corresponding retinal points are seen as single. This fact is explained upon the hypothesis that there are corresponding fusional areas (Panum's areas[7]) around each pair of corresponding points. If images of the same object lie within these areas, the object will appear as single. The neurological arrangement making this possible may be as follows. In addition to the primary nerve connection of each corresponding retinal point to one common brain center, there may also be secondary connections to an area around this common center. In Fig. 11 these areas of secondary connections are schematically shown at A and

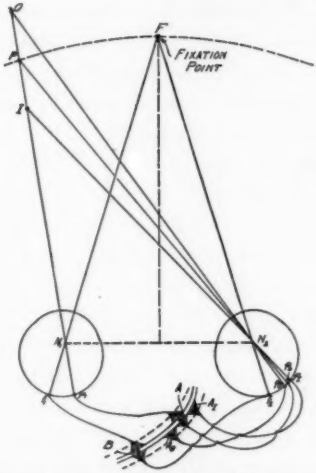

FIG. 11. *Schematic representation of a possible anatomical arrangement explaining the fusional areas.*

B by spreading lines. Assume p_1p_2 represent corresponding retinal points connected with brain center A, and P_0 is connected to brain center A_0 and P_I to brain center A_I. Now p_1 and p_0 are not corresponding retinal points, but if secondary nerve connections from p_1 (at A) overlap those from p_0 (at A_0) then an object that is imaged at p_1 and p_0 will appear as single. Although such an object appears single it will appear farther or nearer than the object whose images stimulate exactly corresponding elements. The extent of this difference in distance depends, if empirical factors are excluded, upon the angular disparity of the images to corresponding retinal points. This explanation is only schematic and an equally good one can be given on the assumption that the areas of

[7] Panum, Arch. f. O.G. *5*, pp. 1–36; 1859, also (Kiel, 1858).

secondary neurological connection are in the retinal layers instead of in the cerebral cortex.

Such hypotheses serve well for an introductory concept of binocular fusion and perhaps depth localization but on further analysis, the capacity to see objects as single in stereoscopic relief is not quite so simple as it might appear, and to explain it a modification of the law of constancy of directional value from excitation of the same brain center is necessary. For example, in Fig. 12 let the eyes be fixated on F, and let A be a point in front of F at such a distance that if an object is placed there its images

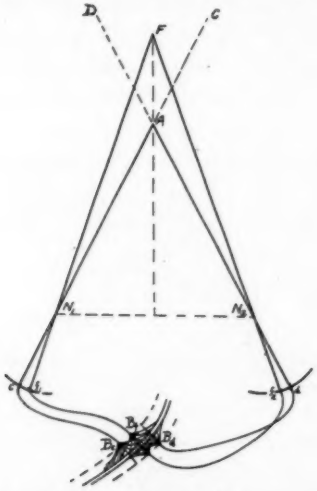

FIG. 12. *Schematic representation of a possible anatomical arrangement for explaining the directional value associated with fused disparate images.*

d and c in the two eyes lie within corresponding fusional areas. If an object placed at A is seen by the O.S. only, it will appear to the right of F at C, due to the stimulation of brain center B_c. This is in conformity with the law that particular directional values result from exciting particular brain centers. If A is seen only with the O.D. it will appear to the left of A at D as would result from stimulating brain center B_d. If an object at A is seen by both eyes and is fused so as to appear singly its directional value is no longer as if from B_c or B_d but from an intermediate point, presumably from B_f; at the same time it appears not at the intersection of the projection of the directional value B_f but at A, the intersection of the projections of the directional values B_c and B_d. That is, fused disparate images are not seen in the directions of the two

brain centers that are primarily stimulated, but in the direction of a single brain center that lies within the corresponding fusional areas some where between.[8]

The explanation of this apparently anomalous phenomenon of an object having an apparent direction as if from one point in space and appearing at a different distance than that point, may be that advanced by Verhoeff[3] which is as follows: When the images of an object that are not formed on corresponding retinal points are fused, three sources of excitation exist at the cortical centers. The first, at the point stimulated by the primary nerve connection from one eye; the second, at the point stimulated by the primary nerve connection of the other eye and the third, at an intermediary brain point. For the object to be seen as single the third excitation would have to be the dominant one, the first and second being suppressed. Though suppressed, the first and second give the directional value to the dominant third excitation. In the ordinary use of the eyes no conflict arises from the directional value of the third excitation since it results not from a direct stimulation from either eye but from a combination of stimulations from both and thus assumes a cyclopean aspect, rather than referring to each eye. But being an excitation of a particular brain center, and due to existing primary nerve connections from that center to each eye, it will have, when attention is called to it, a particular directional value for each eye. Attention can be called to the directional value of a fused image resulting from the excitation of non-corresponding brain centers by placing monocularly seen objects so that their images have the same disparity as the fused images, taking care that they are not associated with the fused image by configuration. The monocularly seen objects will be projected in a different direction from the binocularly seen fused object. The monocularly seen objects will, so to speak, be projected in their true direction, the fused object in the direction of the intersect of the optical projection of the nearest pair of corresponding points.

This is the explanation of the phenomenon which this laboratory has previously described as "retinal slip" where, due to a mispointing of the eyes, the fixation object is imaged on non-corresponding retinal points, and non-fusing dissimilar objects which are so placed that their images have the same disparity as those of the fused objects, appear displaced. The experiment of Panum's limiting case appears to be a particular example of the so-called retinal slip phenomenon, as will be explained later. In view of the above it would seem that the term "retinal slip"

[8] That such is in fact the direction of projection of fused objects will be shown later.

to describe the phenomenon is not satisfactory. "Fixation disparity" would seem more suitable and for want of something better will be used from now on.

III. DESCRIPTION OF APPARATUS

There are four criteria according to Tschermak, for determining the horopter.[9]

(1) The criterion of "median single vision." That is, a determination of the position in space of the surface that lies in the center of the region within which objects are seen as single.

(2) The criterion of the "apparent frontal parallel plane." That is, a determination of the position in space of the surface upon which all objects appear to be in a frontal parallel plane through the fixation point. (Hering's rule.)

(3) The criterion of constancy of "visual direction," that is, a determination of the position in space of the surface upon which objects as seen by each eye appear to be in the same direction.

(4) The criterion of the "maximal differential sensibility to depth." That is, the determination of the position in space from which slight variations in depth are perceived most readily.

Of these four criteria, Tschermak considers the third, i.e., that of constancy of visual direction, the most reliable. It is also consistent with the conception of fixed elementary mutuality of visual direction. The first criterion, that of median single vision and the fourth, that of maximal differential sensibility, he considers less reliable than the two other criteria.[10]

The results presented in this paper are based on a very considerable number of determinations made both by the criterion of the apparent frontal plane and with a specially designed apparatus, by the criterion of the constancy of visual direction.

The apparatus has evolved from that developed by Tschermak and described in his paper "Fortgesetzte Studien über Binokularsehen."[11] An exact duplicate of Tschermak's apparatus was first made and used for some months with satisfactory results. As the work progressed, however, it became evident that improvements, some of which were

[9] Reference 2, page 894.

[10] Determinations made here by the first criterion, i.e., of "median single vision" are described in *Size and Shape of Ocular Images*, Part III (reference 1) and later in this paper. It is believed that the findings indicate that this criterion may be somewhat more accurate than it has heretofore been considered.

[11] Tschermak, Pflügers Arch. *204*, 177–202; 1924.

suggested by Tschermak[12] were necessary. A new apparatus was therefore designed, with two principal purposes in mind; first, to enable determinations of the longitudinal horopter to be made at various fixation distances; second, to enable them to be made more quickly and easily. Various other minor improvements were embodied, the nature of which will appear later.

In order that the determinations could be made at different distances, the apparatus was designed in two parts, *viz.*, one for determinations at distances of from 20 cm to 100 cm and the other for determinations at a distance of 6.1 m. The former will be described first.

A. APPARATUS FOR HOROPTER DETERMINATIONS AT NEAR

In detail, the apparatus consists of thirteen steel ways so mounted on a framework that they all converge to a point, which when the observer's head is adjusted, lies half-way between the mean nodal points of the two eyes, i.e., the observer's cyclopean perspectival center. The central way or lane is perpendicular to the line joining the mean nodal points of the two eyes, thus insuring symmetrical convergence. On each side of this there are six other ways, forming angles of 1°, 2°, 4°, 8°, 12° and 16° to the central one, see *A*, Fig. 13.

In each of these ways, which are 70 cm long, there is a channel 16 mm deep and 0.75 mm wide. A steel strip, *C*, 62 cm long, 24 mm deep and 0.70 mm thick, slides smoothly in each of the channels. It is upon these steel strips that the supports are mounted for the vertical steel wires which are the visual objects used to determine the position of points on the horopter. These steel wires take the place of the plumb threads of Tschermak's apparatus. These supports are shown in *D* and *E*. They consist of two parts, a rear or fixed part, see *a*, which can be clamped on the strip *C*, and a front part, see *b*, which is fastened to *a* by a hinge so that it can be tipped back out of the field of view as shown in *E*. On the front or hinged part, steel rods are attached by means of set screws. Three sets of wire supports are used for three different distances from the observer, *viz.*, 20 cm (5 *D*), 40 cm (2.5 *D*), and 76.5 cm (1.33 *D*). These three distances are chosen to give equal angles of rotation of the eyes in convergence from one distance to the next. When determining the horopter at any one of these distances the vertical rods at the other distances are laid back out of sight, see *E*. The diameter of the steel wires used at 20 cm distance is 0.14 mm, their length 3.1 cm; the diameter of those used at 40 cm distance 0.32 mm, their length 6

[12] Reference 11, p. 185.

cm; the diameter of those used at 76 cm distance 0.60 mm, their length 11 cm. To facilitate fusion and accurately hold fixation, small squares with a pin hole at the center are attached to the center wires.

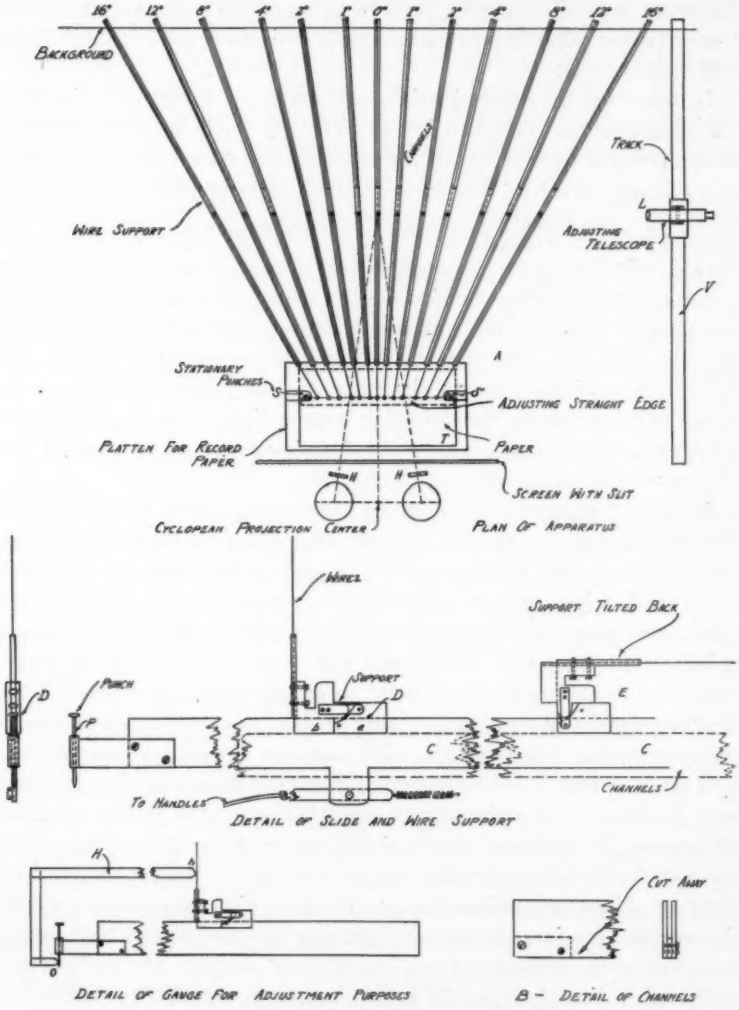

FIG. 13. *Details of the near horopter apparatus.*

Near the middle of the ways *B*, the bottom of the channel is cut away, see *F*, so that projections on the strips *C* may extend below the

ways. To these projections wires are attached. On the other end of these wires conveniently placed handles enable the observer to move the vertical observation wires forward and back along the ways.

The sliding strips *C*, extend in front of the ways. On the front end of each, a small punch *P* is attached. Directly below these punches is a small table, see *T*, upon which a piece of paper can be held, upon which a record of the settings can be obtained by pressing down the little punches and pricking the paper. The center wire with its strip and punch remains fixed. The position of the frontal plane is indicated by the line passing through the prick marks made by the punch on the center strip and those made by two other stationary punches properly positioned on each side of the table at *S* and *S'*, see *A*, Fig. 13. The data recorded for each wire is the distance from the line determined by the fixed punches to the prick marks made by the punches attached to the movable wires. The reading of these data is facilitated by the use of a piece of transparent celluloid that has been accurately ruled with fine lines 0.50 mm apart.

The adjustment of the wires relative to the punches and in a frontal parallel plane is accomplished as follows. First, a straight edge is clamped against the points *SS'*, see *A*, parallel to frontal plane. The punch on the center strip *C* is brought in contact with the straight edge and locked in that position. The vertical wire on this same center strip is placed at the desired distance. The punches on the other strips are then brought in contact with the straight edge and the carrier on each strip is adjusted until all the wires are in a frontal plane parallel to the straight edge. This is accurately done by means of a telescope *L* mounted on track *V*, which is adjusted so that its axis is parallel to the straight edge at *SS'*. The various wires are so adjusted that they fall on the vertical cross hair in the eyepiece of the telescope. It is found that by this method the wires can be adjusted correctly to less than 0.1 mm. Another method for adjusting the wires is by means of a gauge with two parallel edges, see *H*. The edge *O*, is brought in contact with the punches *SS'*, and the gauge clamped. The punches on the other slides are brought up against the edge *O* and then the carriers on the slides so positioned that the wires just touch the other edge of the gauge at *h*.

Empirical factors for depth localization other than those of binocular vision are excluded by the observer's looking through a slit 12.5 cm long and one 8 mm wide in a screen at about 10 cm from the cyclopean point. Behind the wires a larger illuminated background is placed.

There are means for properly positioning and holding the head which

are described later. Lens holders are mounted near the anterior focal point of the observer. This whole horopter apparatus may be set up in conjunction with a haploscope with half silvered mirrors[13] which make it possible to check the accommodative condition while the horopter is being determined.[14]

The apparatus as described is adapted for determining the horopter by the criteria of the frontal parallel plane, median single vision, and maximum differential sensibility. To use it for horopter determinations by the criterion of constancy of visual direction, certain modifications are necessary.

The method of determining the position of objects in space which appear to both eyes to have the same separation is as follows. With the fixation of both eyes held at one point, determinations are made of the angular position of monocularly seen peripherally situated objects which appear to both eyes to have the same separation from the fixation point. For instance, see Fig. 14. Suppose that both eyes fixate on the

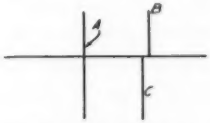

FIG. 14. *The nonius method.*

object A, and that the object B can be seen only by the right eye and the object C by the left. When B and C are so placed as to appear to both eyes at the same distance from A, then images will fall on corresponding retinal points. In a set-up suitable for such determinations there must be means to move B or C laterally to each other and to accurately determine their angular distance from A.

With slight modifications the horopter apparatus is peculiarly well adapted for such determinations. With fixation on the central wire of a horopter apparatus, a forward or backward movement of one of the lateral wires decreases its angular distance from the fixation wire from the point of view of one eye and increases it for the other. The only alteration of the horopter apparatus that is necessary is means to allow the upper part of the thread to be seen by one eye only and the lower part by the other eye only. This can be accomplished by screens properly placed before the eyes.

[13] See *Ocular Measurements*, (reference 1).

[14] The inclusion of these mirrors necessitates a correction of the data recorded since an unequal displacement of the apparent positions of the wires takes place across the visual field.

Fig. 15 is a diagrammatic plan of the apparatus with this adaptation. Vertical wires can be moved along lanes that converge on the cyclopean nodal point. Screens (see Fig. 16) are so placed before the eyes that while allowing the fixation target at A to be seen by both eyes, they affect the appearance of the lateral wires at the right and at the left

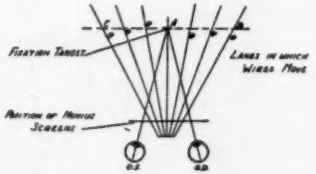

FIG. 15. *Plan of the horopter apparatus when grid-nonius method is used.*

of A, as follows. The O.D. can see only the upper half of the lateral wires at the right of A, Fig. 15, which the grid causes to appear as dashed lines (see b, Fig. 17)—and the lower half of the lateral wires at the left of A which appear as solid lines (see c', Fig. 17). The O.S. sees only the lower half of the lateral wires at the right of A which appear as solid lines (see c, Fig. 17) and the upper half of those at the left of A

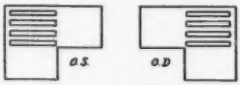

FIG. 16. *Screens used in the grid-nonius device.*

which appear as dashed lines (see b', Fig. 17). The observer fixates on a square at A. By means of convenient handles he moves the wires forward and backward causing the dash and solid lines to appear to move laterally relative to each other. (See b, c and b', c', Figs. 17 and 18.)

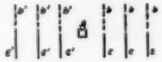

FIG. 17. *Appearance of the wires in the horopter apparatus when adjusted in the nonius method.*

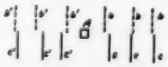

FIG. 18. *The appearance of the wires of the horopter apparatus when not adjusted in the nonius method.*

While maintaining his fixation at A he adjusts them until they are collinear, i.e., the dash line is a continuation of the solid line. The position of a wire when so adjusted gives a measure of the difference in the

angular position of the projections of corresponding retinal points of the two eyes from the points of fixation for that particular peripheral angle. Since the lateral displacement is small relative to the forward and backward movement a large leverage is obtained, making a very

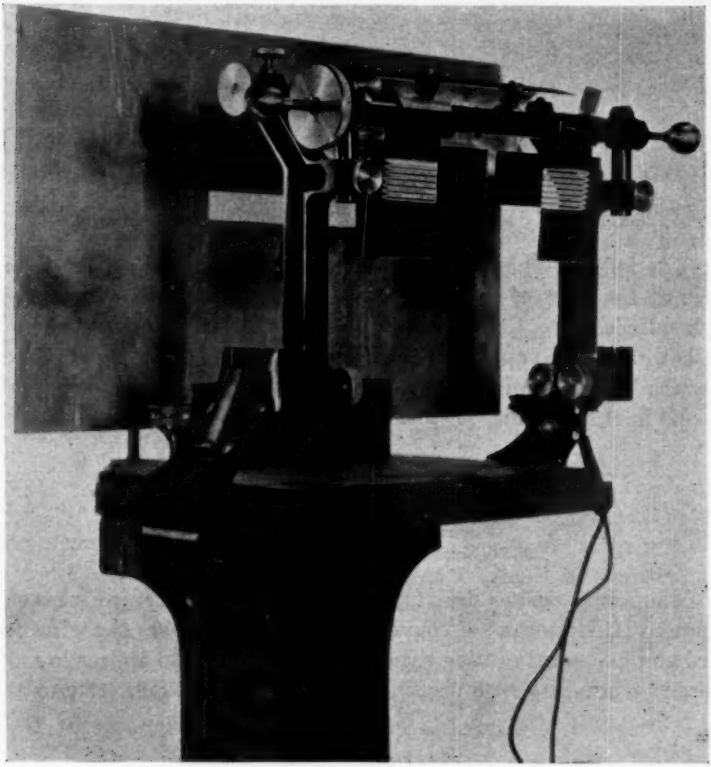

FIG. 19. *Photograph of the grid-nonius apparatus. (Rear view.)*

sensitive adjustment possible. It has been found that with this method more accurate settings can be made if the diameter of the peripherally seen wires is increased. By an adjustment of the whole series, measurements are obtained for a number of different peripheral angles. The term "grid-nonius horopter"[15] is used to describe this method. Fig. 19 is a photograph of the grid attachment as used. Two electric lamps

[15] The above described arrangement is a development and improvement of Tschermak's nonius method. See F. P. Fischer: Fortgesetzte Studien über Binokularsehen. III. Mitt.

illuminate the grids. The grids are fastened to carriers that slide along a bearing. When the grids are in a position to give solid and broken lines near the fixation point the limit of the visible field is about 10° on each side. Due to the interocular distance and the distance at which the grid must be from the eyes this limit cannot be extended. To get horopter determinations beyond this limit the grids are pulled out along the bearing a required amount. The illumination on the screens must be such that they merge with the background.

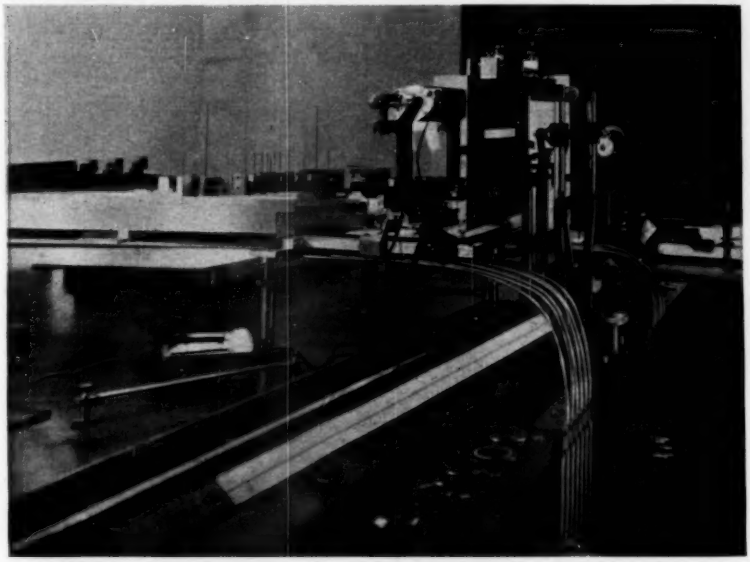

FIG. 20. *Photograph of the near horopter apparatus, showing adjustment for 2.5 D., with grid-nonius device in place.*

In general the procedure is the same as that used in horopter settings on the criterion of the frontal plane. Great care must be taken to hold the fixation exactly.

B. APPARATUS FOR HOROPTER DETERMINATIONS AT A DISTANCE

The distant horopter apparatus is a duplication on a large scale of that used at near. A large table was set up across the room so that its center was 6.1 m or twenty feet from the first principal point of the ob-

Pflügers Arch. *204*, pp. 234–246; 1924. It is in part similar to Tschermak's method and in fact resulted from the use of that method. The differences between the two methods as well as the difference in results obtained will be described fully later.

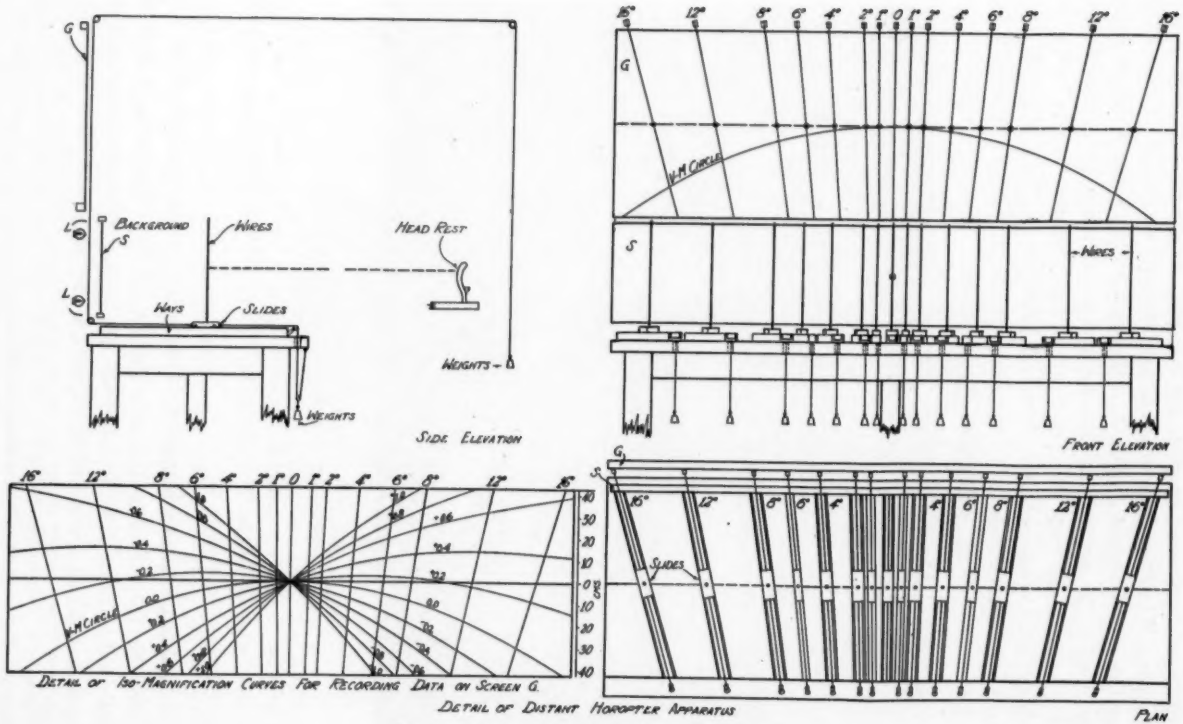

FIG. 21. *Details of the 6.1 meter horopter apparatus.*

server's eyes. On this table was placed a series of wooden tracks, 1.5 m long, in line with and forming the same angles as the ways on the near apparatus. On these tracks were wooden slides (travelling on small brass wheels) which supported vertical rods 90 cm long and 4 mm in diameter.

The position of these slides can be controlled by the observer by means of cords and weights arranged as follows. On the front of each slide, cords were attached which pass over pulleys at the front edge of the table. On the end of the cords are weights sufficient to pull the slides forward, see Fig. 21. On the rear of each slide cords are attached which pass under pulleys at the back edge of the table then up behind a transparent screen *S* and in front of another screen *G* and over pulleys near

FIG. 22. *Photograph of the distant horopter apparatus.*

the ceiling, then across the ceiling and down over pulleys to a position within convenient reach of the observer. To the end of these cords weights are attached which balance the weights above mentioned. When the observer pulls down or releases these cords the rods on the carriers move forward and back along the slides and stop in any position they may be in when the cord is released. Back of the rods is a transparent screen *S* which is illuminated by a double row of electric lights *L*.

To facilitate the reading of the position of the setting of the rods the following arrangement is used. Above the screen *S* and invisible to the observer while making settings, is placed another screen *G*, 4.5 m long,

1.3 m wide representing a plan of the table. In front of it pass the above described control cords, on each of which are fastened small wooden balls 8 mm in diameter as indicators. The position of the small balls on the screen tells the position of the vertical rods relative to the normal plane. When the observer takes his head from behind the apparatus, he can read off his settings without moving. There are several types of scales which might be used on the screen by which the position of wires can be recorded. The type adopted is that shown in Fig. 21. It is a series of iso-magnification curves (to be described later) which gives the percentage difference between the angles of a given peripheral wire from the fixation point, as seen by the two eyes. The reasons for using this type of scale will appear later.

The grid-nonius method above described cannot be used at a distance of 6.1 m due to the fact that at that distance the lateral movement resulting from the limited forward and backward movement is too small.

With the above described set-up it is possible to determine the position of the horopter at various distances. Moreover, the means of recording and reading the settings not only greatly speeded up the work, but also made it possible for one person to both make the settings and record the data with ease and without fatigue. By putting lenses in the lens holders *H* the condition of phoria, refraction, and size and shape of the dioptric images can be varied. At the same time the actual condition of phoria and refraction can be determined by the haploscopic attachment.

With the present apparatus it is not possible to determine the relative space relationships that exist between various projections of corresponding retinal points (see page 574). A new apparatus is under construction which will make such determinations possible at the same time that the projections of corresponding retinal points are being determined. This is accomplished by adjusting the tracks of the apparatus laterally as suggested by Tschermak.

IV. EXPERIMENTAL PROCEDURE

The observer's head is correctly positioned so that he converges symmetrically on the fixation wire and that the center to which the ways converge lies directly below the midpoint of the line joining his mean nodal points. This is accomplished as follows. The centers of rotation of the arms of the haploscope, which are part of the apparatus, are separated for his interpupillary distance. The arms of the haploscope are set for the convergence being used. Centered pinhole diaphragms

are then placed in lens holders which are attached to the arms of the haploscope at the anterior focal point of the eyes. The head is then fixed in the headrest so that the observer can see the fixation wire in the middle of each pinhole. This insures correct lateral positioning of the head. The correct forward and back position of the eyes is determined by aligning the front surfaces of both corneas with small sights attached to the headrest which are parallel with the fixed frontal parallel plane. When the corneas are in this position the first principal points of the eyes are at the required distance from the fixation wire.[16]

The experimental data were taken for black wires against a white background (cf. Tschermak's black horopter). The general illumination in the room where the measurements were made was from the daylight which came in from large windows on one side. The background against which the wires were seen was white and kept at a uniform and constant illumination of from 30 to 65 foot candles by electric lights screened from the observer.

While setting the wires great care was taken to keep an exact fixation. This was facilitated by the fixation object described in which the small pinhole appeared like a fine bright star.

The usual procedure was to set the wires nearest the fixation wire, one on one side and then the nearest one on the other. No difference in settings could be found whether the nearest or most peripheral wires or those all on one side were set first.

All settings were made by the observer himself. To avoid any possibility of the observer kinesthetically affecting his settings the handles

[16] K. N. Ogle, *An Analytical Treatment of the Longitudinal Horopter: Its Measurement and Application to Related Phenomena, especially to the Relative Size and Shape of the Ocular Images.* (To be published.) It is of importance to know just how accurately the eyes must be positioned. A mathematical study was made of the nature of the variation of the horopter that would result if the eyes were not in the proper position. In general considerable displacement of both eyes equally either forward or back has only a second order effect on the position of the horopter. If however the eyes are not parallel with the frontal parallel plane, for example, if the head were slightly rotated about a vertical axis, a considerable change in the position of the horopter may result. The horopter will take a position as if rotated about a vertical axis the same number of degrees that the head is rotated. The displacement of one eye forward and the other eye back of one mm with a P.D. of 65 mm is equivalent to a rotation of 1.7° which would amount to an error in percentage size between the two eyes of about 0.47 percent at 40 cm, and 0.09 percent at 20 cm, and 0.03 percent at 6 cm. Great care must therefore be taken that the poles of the two corneas lie in a plane parallel to the fixation frontal plane and so remain throughout the determinations. Another type of variation is introduced by lateral displacement of the eyes. Such displacement has a similar effect to that of rotating the head. For a given displacement however the effect is much less, a lateral displacement of 1 mm being equivalent to a rotation of only about 0.12° at 40 cm.

by which the wires were controlled were staggered. That the settings were in fact not influenced by such effects was evidenced by the consistency of results obtained when lenses which changed the size by a-amounts unknown to the observer were placed before his eyes.

A number of settings were taken at one sitting. These were recorded by punch pricks in a paper which was moved along on the carrier as described, between each setting.

A series of settings having been obtained, their distances from the fronto-parallel plane were determined by measuring the distances of the punch marks from lines parallel to the frontal parallel plane drawn through the fixation punch mark. These distances for each peripheral angle were averaged and the mean deviation computed.

V. METHOD OF ANALYZING EMPIRICAL DATA

Since the approach to the investigation was from the point of view of the physiological importance of the relative size and shape of the ocular images, it was necessary to devise methods of analyzing the results so that information concerning these images might be obtained.

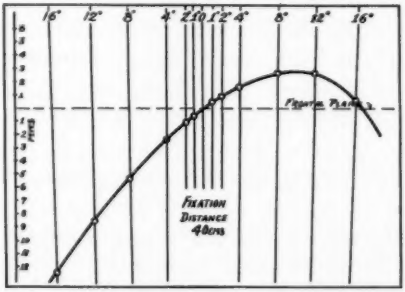

FIG. 23. *Graphical representation of schematic data in a spatial graph (cf. Tschermak).*

Horopter determinations may have been made by any of the criteria described above. The data found are averages of a number of determinations of the positions of the wires in the various lanes recorded in mm as the distances from the fixation frontal plane, for example, Table 1. Distances behind the frontal plane are regarded as positive and those nearer as negative. Such data can be put in representative graph form as Tschermak has done (Fig. 23). The straight dotted horizontal line represents the fixation frontal plane, the slanted vertical lines represent the lanes in which the wires move. The vertical scale has been magnified ten times. The positions of the points in the graph of the horopter are

found by measuring the values obtained along their respective lanes. A line connecting these points represents the trace of the horopter.

TABLE 1.

Field	Left field						F	Right field					
Lane	16°	12°	8°	4°	2°	1°	0°	1°	2°	4°	8°	12°	16°
Distance of wire from frontal plane mm	−12.6	−8.8	−5.1	−2.1	−1.0	−0.5	—	0.4	0.8	1.3	2.0	2.2	0.8
Transformation values in percent	−2.70	−1.70	−0.77	0.11	0.56	0.80	—	1.25	1.45	1.90	2.86	3.86	4.82

As has been pointed out, there is a correlation between the size and shape of ocular images and the position and shape of the horopter. For

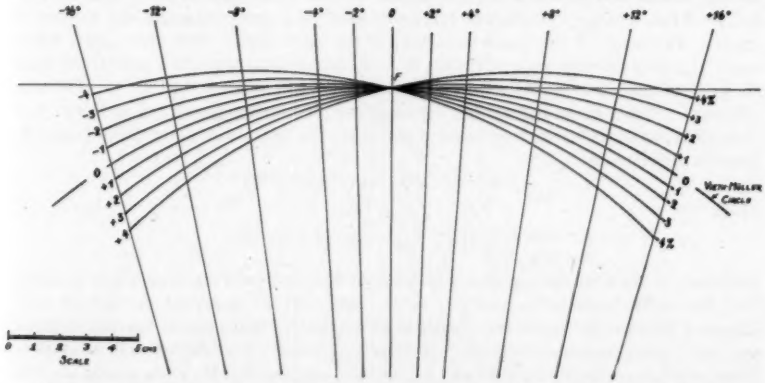

FIG. 24. *Illustration of the iso-magnification curves for a fixation distance of 40 cm.*

instance, if the horopter lies on the Vieth-Müller circle, the ocular images in both eyes are identical; if the horopter takes a position as if rotated about the fixation point, the ocular image of one eye is larger than that of the other. The first problem was to determine the magnitude of the percent difference in the size of ocular images associated with determined positions of the horopter. This was accomplished as follows. A graph was made on which were plotted the positions that a series of horopter traces would take if the relative size of equal ocular images were made different by fractional units of percent. These gave what might be called iso-magnification curves. Fig. 24 shows such a series

when the fixation intersect is at a distance of 40 cm and the P.D. is 65 mm. Fig. 25 shows a similar set when the fixation intersect is at a distance of 6.1 meters or twenty feet. The curve marked 0 percent is the Vieth-Müller circle, all points on which subtend equal angles to each eye. The curve marked +1 percent gives the loci of the points in space which subtend angles to the O.D., which are 1 percent greater than they subtend to the O.S., etc. The curves marked with a minus (−) sign are the loci of points that subtend smaller angles to the O.D. by the percents indicated. It is of interest to note how differently these iso-magnification curves are positioned relative to the frontal plane in the 20 feet graph and the 40 cm graph. By interpreting empirical data against the iso-magnification curves by plotting them on the same graph, it is possible to read off the approximate magnitude of the difference in the size of the ocular images for any given peripheral angle.[17] To illus-

[17] In detail, the method of handling the data is as follows. The empirical data give the average distances in mm from the frontal plane at which the wires on the various lanes are set, see Table 1. When so positioned every wire subtends a particular angle with the lines of fixation of each eye. If the wire is positioned on the Vieth-Müller circle these angles will be equal. If it is on the right-hand side of the field and farther away than the Vieth-Müller circle, the angle subtended to the O.D. will be larger than that subtended to the O.S., etc. The exact difference between the angles can be calculated from the known distance of each wire from the frontal plane and the angle of the particular lane. The formula for determining these relations for each lane, is

$$(y-b)=(1/2P)\ \{S+(S^2+4Pa^2)^{1/2}\}$$

where

$$P=(\tan\phi)^2-[\frac{e}{2+e}\ \frac{a^2+b^2}{ab}]\tan(\phi+2)$$
$$S=(b^2-a^2)/b$$

and where $(y-b)$ is the distance of a point from the fixation frontal plane, on a lane, ϕ degrees from the median plane taken positively for the right field and negatively for the left, for a difference between the longitudinal angles of 100e percent. b and a are the fixation (distance) and nodal point base line distances, respectively. To avoid the delay of such calculations, transformation graphs for the right and left field are used, see Fig. 28. These graphs are computed from the above formula. Distances nearer and farther than the frontal plane are marked on the abscissa axis, nearer distances minus (−) and farther distances plus (+). Percent differences in size of the angles subtended to each eye are marked on the ordinate axis, plus (+) if the angle subtended to the O.D. is larger than to the O.S., and minus (−) if it is smaller. The slanting lines marked 1° and 2°, etc., represent the lanes. An example of the transformation process is as follows: At 4° in the right field the average setting of the wire in the right field was 1.7 mm behind the frontal plane. Following the 4° lane on the graph for the right field to a point 1.7 mm to the right of the ordinate axis one refers to the ordinate axis and reads +2.1 percent. This indicates that the angle subtended to the O.D. by that particular point is 2.1 percent larger than that to the O.S. This is then plotted on the analytical graph, see Fig. 27, at 4° on the abscissa to the right of the vertical axis and at the 2.1 percent mark on the ordinate above the horizontal axis. The other data are plotted in the same way. Different interpolating graphs must be used for each different distance, and theoretically for every different interpupillary distance. Interpupillary differences of three mm each way introduce such slight variations, however, that they can be neglected. [Cf. reference 16.]

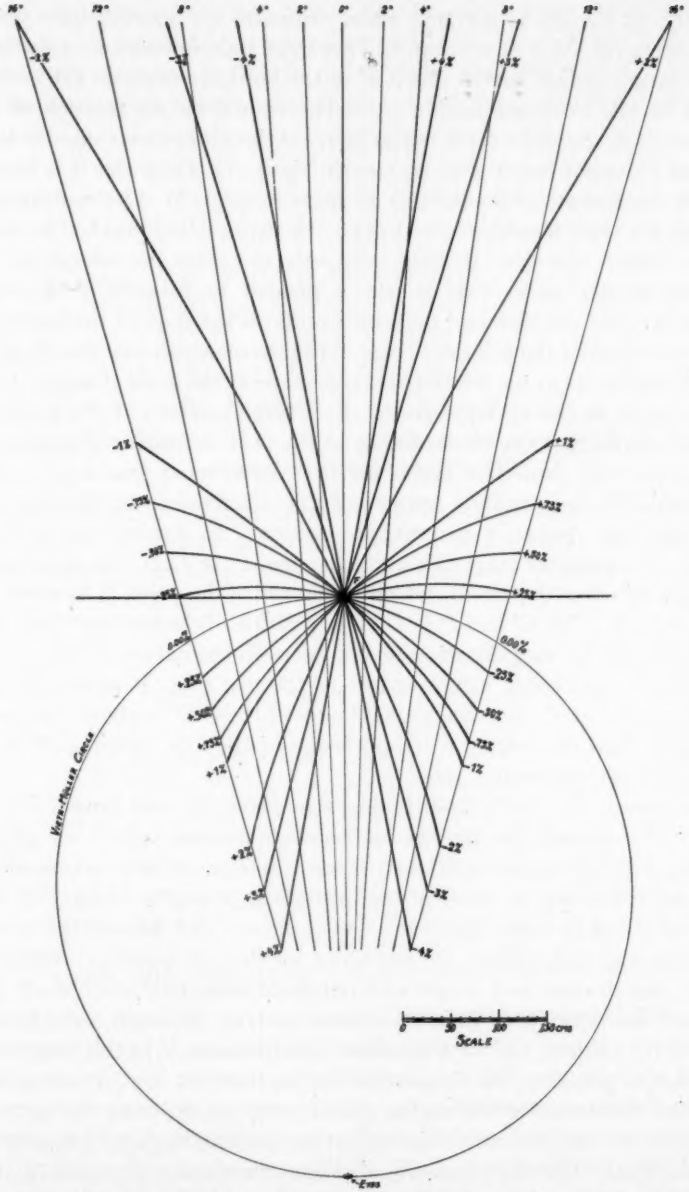

FIG. 25. *Illustration of the iso-magnification curves for a fixation distance of 6.1 meters.*

trate, let Fig. 26 be a graph, whose ordinates are magnified ten times, showing the trace of an empirical horopter superimposed on a series of iso-magnification curves. Point *B* of the horopter trace on the 4° lane lies on the iso-magnification curve that would be the position of the trace of the horopter if the ocular image of the left eye were slightly more than 2 percent larger than that of the right eye. From this it is known that the distance *FB* subtends an angle to the O.D. 2 percent greater than the angle it subtends to the O.S. The angle subtended by the point *C* is almost the same to both eyes since the point lies almost on the Vieth-Müller circle, that is, the 0 percent iso-magnification curve. Similar data can be found for other points on the trace of the horopter. The relation of the horopter trace to the iso-magnification curves gives information as to the relative size and shape of the ocular images of the two eyes. In the example given, the rotated position of the horopter trace shows that the ocular image of the O.D. is smaller than that of the O.S.—the projection fan of the O.D. being more spread out or extended. The quantitative amount of this difference in size is given by the average change in percent size necessary to remove the rotation from the horopter trace. This will happen if the O.D. image is made larger by about 1 percent, which would cause the point *B* to move to *B'*, *A* to *A'*, *C* to *C'* and *D* to *D'*. The position of the horopter trace relative to the iso-magnification curves also tells the nature of the asymmetrical relationship of the images of the two eyes. It shows, for instance, that at 4° the nasal retinal image of the O.D. is about 1 percent smaller than the temporal retinal image of the O.S.; while at 8° it is about 2 percent smaller, etc.

Although this use of iso-magnification curves is most productive, it not only necessitates the use of iso-magnification curves for graph paper, but fails to give sufficiently quantitative or complete information. To meet this need, a study of the theoretical principles underlying the horopter and its variations in relation to the size and shape of the ocular images was undertaken. An improved method of graphing empirical data was devised and a new and improved analytical method of approach was developed. This was imperative for a thorough understanding of the subject, and for a solution of its problems.[17] In this improved method of graphing, the data are plotted as shown in Fig. 27, where the percent differences in the angles, which points on the horopter subtend to each eye, are plotted on the ordinates against the peripheral angles as abscissae. The angles on the abscissae are those subtended to the O.D. The ordinate above the axis gives percent differences in angular

size when the O.D. is larger than the O.S.; that below the axis, when the angle to the O.D. is smaller than that to the O.S. The points *A*, *B*, *C*, *D* in Fig. 26 when so plotted will take the positions indicated Fig. 27. The trace connecting them will give a curve representing a horopter

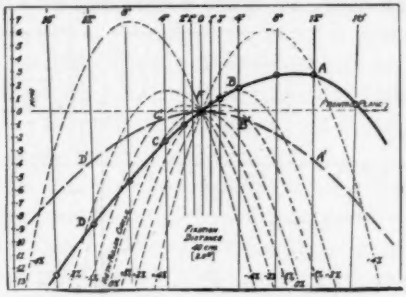

FIG. 26. *Graphical representation of the same schematic data in a spatial graph on which the iso-magnification curves are shown.*

trace in terms of percent differences of the angles which the points of the horopter subtend to each eye.[17] The special features of the analytical graph related to the spatial one are: (1) The Vieth-Müller circle coincides

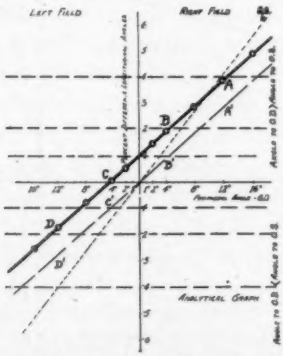

FIG. 27. *Graphical representation of the same schematic data in an analytical form.*

with the axis of the abscissa, since all points on that circle have zero percent differences between longitudinal angles. (2) The iso-magnification curves become a series of straight lines parallel to the abscissa axis. (3) The left and right halves of both graphs correspond to the left and right visual fields. (4) The data of the "normal" horopter so transformed become a straight line, the slope of which indicates the magnitude (*H*) of the

Hering-Hillebrand deviation,[18] i.e., the unbalanced distortion between the ocular images in the two eyes, or a quantitative measure of the asymmetry in the projection fans for corresponding retinal points. This deviation constant generally varies from 0.00 to 0.35. $H=2a/b$ is that for the fixation frontal plane, $2a$ being the nodal point base line and b the fix-

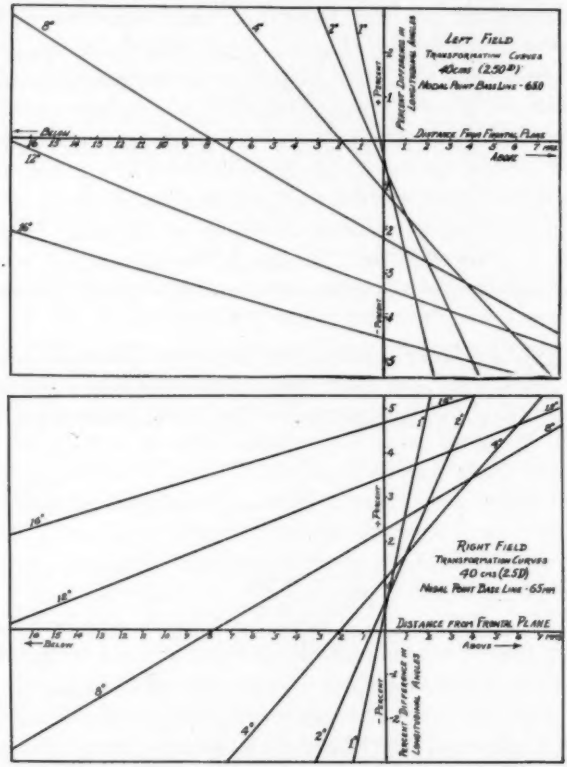

FIG. 28. *The transformation graphs for the right and left fields for the fixation distance of 40 cm.*

ation distance. (5) The overall percent difference between the ocular images of the eyes (assuming symmetrical convergence of the eyes), is given quantitatively by the intersect of the "horopter line" on the ordinate axis.[16] If this value lies above the abscissa axis the angles between the lines

[18] The slope H is usually specified by the ratio of the percent difference of longitudinal angles (expressed in the decimal) relative to the tangent of the peripheral angle of the right eye, for theoretical reasons. The slope expressed otherwise would of course be approximately proportional over the ordinary angles used.

of the projection fan of the right eye are greater than those of the left, if below, the angles between the lines of the projection fan of the right eye are smaller than those of the left eye by the percent indicated. (6) The dotted line shows the slope of those transformed data when the horopter lies in the fixation frontal plane. The slope of this line will be 100 $2a/b$ where $2a$ and b are the mean nodal point base line and fixation distance from the cyclopean projection center, respectively. This slope, of course, refers to percent difference in tangents of longitudinal angles as a function of the tangent of the longitudinal angle to the right eye, for a given point on the longitudinal horopter.

It is evident that this type of graph gives quantitative information as to the relative size and shape of the ocular images that is not apparent in the trace of the horopter. They are in fact direct graphs of the percent differences in the angles formed by optical projections of corresponding retinal points with the fixation projection. In other words, they are graphic representations of the relation of the angles formed by corresponding lines of the projection fans with the fixation lines.

Their significance may be more easily understood if they are considered as graphical representations of the relation between the angles formed by corresponding lines of the projection fans of each eye. Consider the simplest case, where the angles in one projection fan are identical with those of the other (see Fig. 6). The point C has an angle of obliquity of 4°. The relation between the angles $F\ N_1\ C$ and $F\ N_2\ C$ (since these angles are equal), is represented by a point on the abscissa in Fig. 27. Since all the other angles as $F\ N_1\ B$ and $F\ N_2\ B$ are equal, the curve will lie on the abscissa axis. If the corresponding angles are not equal, which is the case when the horopter lies anywhere but on the Vieth-Müller circle, the difference between them in percent is indicated by the points on the graph which correspond to the difference.

Such graphs, however, do not indicate the relative subjective space or directional value associated with the projection of each pair of corresponding points. That is, they do not give the relationship between the angles $F_1N_1A_1$ and $A_1N_1B_1$, etc., as in Fig. 4.

To find these relationships, determinations must be made of the actual separation of a series of objects at the intersects of the projections of corresponding retinal points when they appear equally spaced, so-called multiple partition experiments. Since these objects are imaged on the corresponding points of each eye, the space values as projected from each eye are given by the extent to which such objects do not subtend equal angles to each eye. These differences may be expressed in

terms of percent change in the peripheral angles to the objects, see Fig. 29, where the percent values are plotted on the ordinates magnified ten times against the peripheral angles for the positions of each of the apparently equally spaced objects as abscissae. If such a series of objects at the intersects of projections of corresponding points appear equally spaced, and are in fact equally spaced, the curve will coincide with the abscissa axis. If the angular separation of the points is not equal as in the Kundt and Münsterberg cases, the curves will take some other position and shape. From a graph of this type, in combination with an analytical graph, the relationship between the projections of corresponding retinal points of both eyes is definitely described. A diagrammatic representation of these relationships is given by the projection fans.[16]

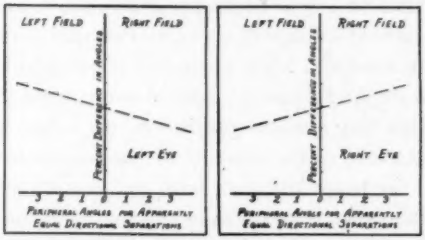
LEFT FIELD
RIGHT FIELD
PERCENT DIFFERENCE IN ANGLES
LEFT EYE
3 2 1 0 1 2 3
PERIPHERAL ANGLES FOR APPARENTLY EQUAL DIRECTIONAL SEPARATIONS
LEFT FIELD
RIGHT FIELD
PERCENT DIFFERENCE IN ANGLES
RIGHT EYE
3 2 1 0 1 2 3
PERIPHERAL ANGLES FOR APPARENTLY EQUAL DIRECTIONAL SEPARATIONS

FIG. 29. *Method of graphical representation of the monocular multiple partition experiments from which the relationship between the projection lines of the fans can be shown.*

The subjective space or directional value associated with the projection of a series of pairs of corresponding points can also be determined as follows. First, the space values for one eye may be obtained by the positioning of a series of points that appear to have the same directional separation. These values are then plotted to give a curve showing the gradient of space across the field. From such a curve and an analytical graph of the horopter the space values in the other eye may be found by eliminating the former from the latter.

The second part of this paper, presenting experimental findings, will appear in the next number of this journal.